works offer insights into the molecular mechanisms by which ATRA exerts its biological effects on neuroblastomas. All-*trans*-retinoic acid activates phosphatidylinositol 3′-kinase-Akt pathway that plays an important role in neuronal differentiation (Encinas *et al.*, 1999; Lopez-Carballo *et al.*, 2002), and it reduces the expression levels of MYCN (Thiele *et al.*, 1985) and upregulates the cyclin-dependent kinase (CDK) inhibitor $p27^{KIP1}$ in association with the ATRA-induced cell cycle arrest in neuroblastoma cells (Lee *et al.*, 1996; Nakamura *et al.*, 2003). In addition, certain neuroblastoma cells underwent apoptosis in response to ATRA (Piacentini *et al.*, 1992; Takada *et al.*, 2001; Nagai *et al.*, 2004). Consistent with these observations, 13-*cis*-RA treatment after intensive chemotherapy improved an event-free survival rate of the patients with aggressive neuroblastomas with 17% increase (Villablanca *et al.*, 1995; Matthay *et al.*, 1999). Although the antitumor effects of RA alone on aggressive neuroblastoma are limited, RA treatment has an advantage that it carries no severe side effects. Thus, it is important to enhance the antitumor effects of RA on neuroblastoma cells, and thereby inducing apoptosis.

In the present study, we have found that the ATRA treatment induces neuronal differentiation in neuroblastoma-derived LA-N-5 and RTBM1 cells, whereas CHP134 and NB-39-nu cells undergo p53-independent apoptotic cell death in response to ATRA. Extensive expression studies revealed that the antiapoptotic Bcl-2 was constitutively expressed at high levels in LA-N-5 and RTBM1 cells, whereas CHP134 and NB-39-nu cells expressed Bcl-2 at extremely low levels. Enforced expression of Bcl-2 in CHP134 cells led to a significant inhibition of the ATRA-mediated apoptosis. In accordance with these results, the treatment with Bcl-2 inhibitor in RTBM1 cells resulted in an increased sensitivity to ATRA. Moreover, two out of 10 sporadic neuroblastomas in primary cultures with undetectable *bcl-2* underwent cell death in response to ATRA, whereas seven tumors out of the remaining eight cases expressed high levels of *bcl-2*. These results suggest that Bcl-2 might be a key regulator for the ATRA-mediated apoptotic cell death in neuroblastomas.

Results

ATRA-induced growth inhibition, differentiation and cell death in human neuroblastoma cell lines

To examine the possible effects of ATRA on growth and viability of neuroblastoma cells, human neuroblastoma-derived LA-N-5, RTBM1, CHP134 and NB-39-nu cells were cultured with or without 5 μM of ATRA, and the numbers of viable cells were counted at the indicated time points after the exposure to ATRA. As shown in Figure 1a, ATRA effectively inhibited proliferation of these neuroblastoma cells. Among them, the growth of CHP134 and NB-39-nu cells was much more suppressed in the presence of ATRA. To monitor morphological changes induced by ATRA, ATRA-treated cells were checked by phase-contrast microscopy. As shown in Figure 1b, a neurite outgrowth was evident in ATRA-treated LA-N-5, RTBM1 and CHP134 cells, whereas it was marginal in NB-39-nu cells. Of note, ATRA-induced cell death was detectable in CHP134 and NB-39-nu cells, but not in LA-N-5 and RTBM1 cells. To confirm whether ATRA could induce the apoptotic cell death in CHP134 and NB-39-nu cells, we examined the changes in the number of cells with sub-G1 DNA content in response to ATRA. As shown in Figure 1c and d, the flow cytometric analysis revealed that the number of CHP134 cells with sub-G1 DNA content was significantly increased in response to ATRA. Similarly, ATRA promoted the apoptotic cell death in NB-39-nu cells, albeit to a lesser degree than CHP134 cells. Under our experimental conditions, ATRA failed to induce the apoptotic cell death in LA-N-5 and RTBM1 cells (data not shown).

ATRA-induced apoptotic cell death in neuroblastoma cells

To elucidate the molecular mechanism(s) underlying the ATRA-mediated apoptotic cell death in neuroblastoma cells, we examined whether the procaspases could be proteolytically cleaved to be activated in response to ATRA. To this end, whole-cell lysates prepared from the indicated neuroblastoma cells exposed to 5 μM of ATRA for 0, 2, 4 and 6 days were subjected to immunoblotting with the indicated antibodies. As shown in Figure 2a, the time-dependent proteolytic cleavage of caspase-9 and caspase-3 was observed in CHP134 and NB-39-nu cells, but not in LA-N-5 and RTBM1 cells. Consistent with these results, one of the physiological substrates of the activated caspase-3, poly-ADP-ribose polymerase (PARP), was cleaved in ATRA-treated CHP134 and NB-39-nu cells. In a good agreement with the previous observations showing that caspase-8 is epigenetically silenced in a high percentage of neuroblastoma cells (Teitz *et al.*, 2000; van Noesel *et al.*, 2003), caspase-8 was undetectable in LA-N-5, RTBM1 and CHP134 cells. In contrast, NB-39-nu cells expressed a large amount of procaspase-8. Procaspase-12, which is involved in the endoplasmic reticulum-stress-induced apoptosis (Nakagawa *et al.*, 2000; Morishima *et al.*, 2002), was readily detectable in all of the neuroblastoma cell lines that we examined, and did not respond to ATRA. Under our experimental conditions, ATRA had negligible effects on proteolytic cleavage of caspase-8 and caspase-12 (data not shown).

As caspase-9 is activated in response to the cytoplasmic release of cytochrome *c* from mitochondria, leading to the activation of caspase-3 (Degterev *et al.*, 2003), we sought to examine whether cytochrome *c* could be released in response to ATRA. To this end, CHP134 cells were treated with 5 μM of ATRA or left untreated, and cells were incubated with the antibody against cytochrome *c* or with the control immunoglobulin (Ig)G. Cell nuclei were stained with 4,6-diamidino-2-phenylindole (DAPI). Microscopic images demonstrated that cytochrome *c* staining displays a punctuate

cytoplasmic pattern in the absence of ATRA (Figure 2b, left). This staining pattern was almost identical to the MitoTracker staining (data not shown). ATRA treatment for 4 days induced redistribution of cytochrome *c* to a diffused cytoplasmic pattern in cells with apoptotic nuclei (Figure 2b, middle), suggesting

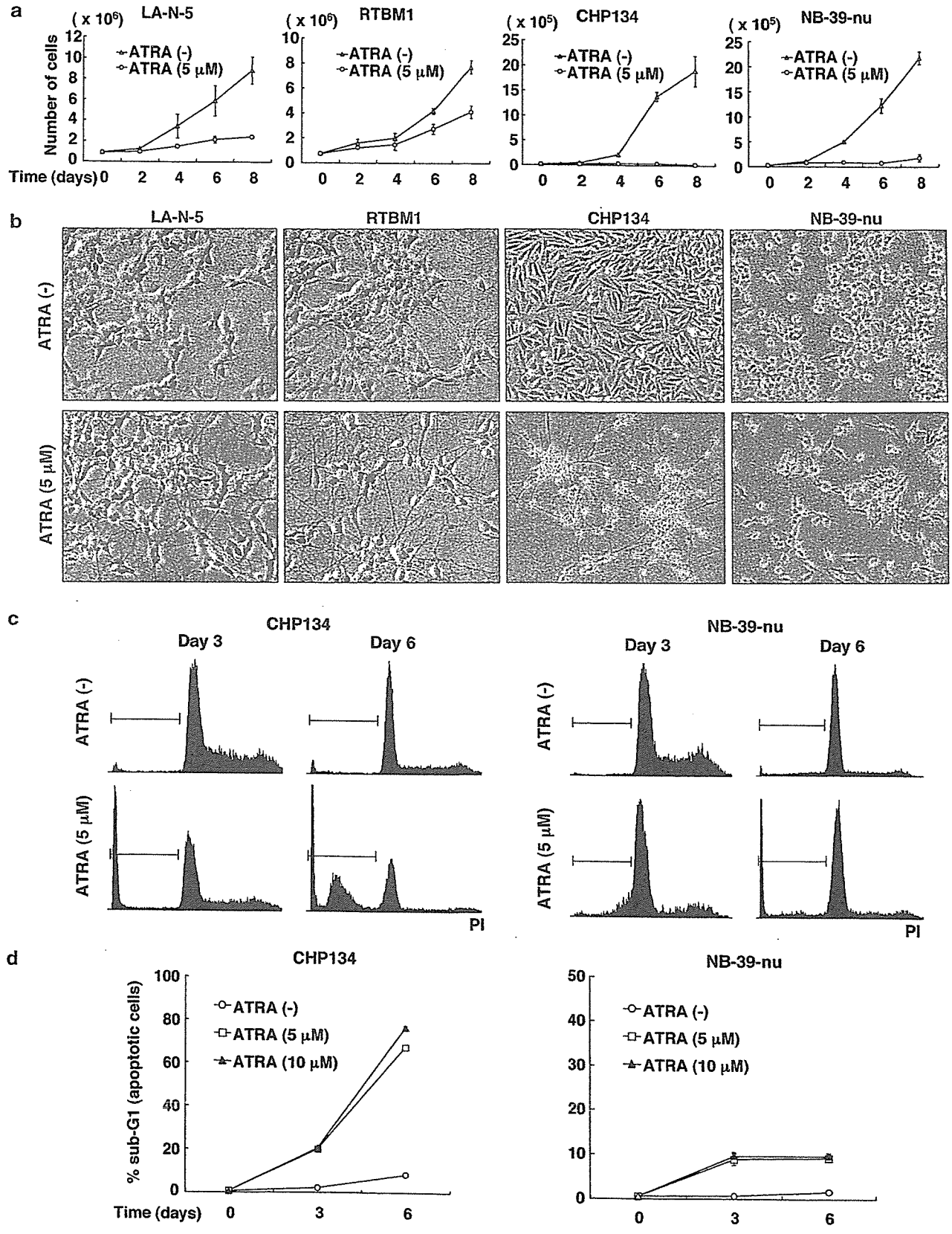

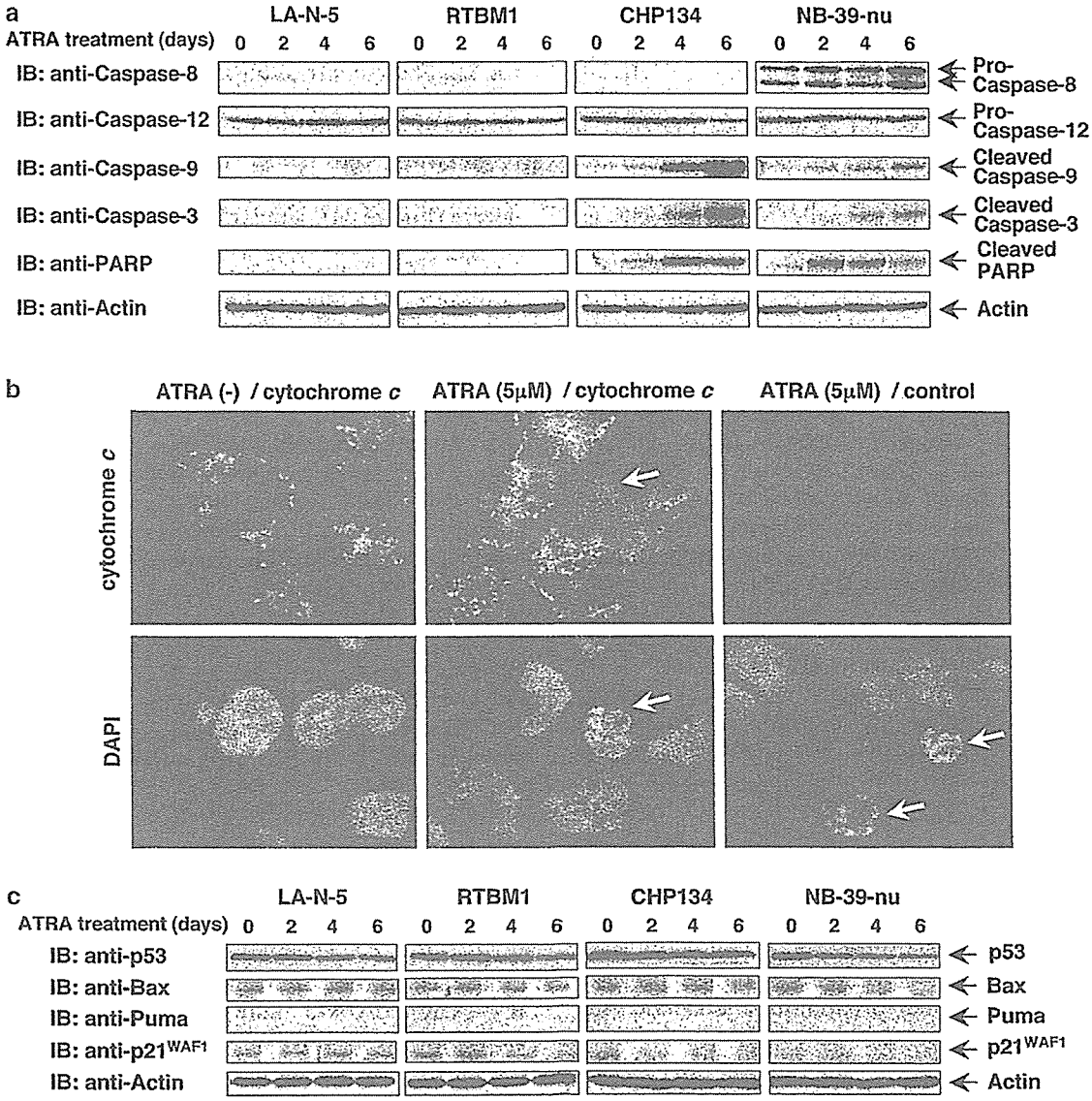

Figure 2 Caspase-9 and caspase-3 are cleaved during the all-*trans* retinoic acid (ATRA)-mediated apoptosis in CHP134 and NB-39-nu cells. (**a**) Immunoblot analysis for various caspases and poly-ADP-ribose polymerase (PARP) in response to ATRA. The indicated neuroblastoma cell lines were treated with 5 μM of ATRA or left untreated. At the indicated time points after the treatment with ATRA, whole-cell lysates were prepared, and analysed by immunoblotting with indicated antibodies. Actin expression was used as a loading control (bottom). (**b**) ATRA-induced cytoplasmic release of cytochrome *c* in CHP134 cells. CHP134 cells were seeded onto coverslips, and cultured in the presence or absence of 5 μM of ATRA. Four days after the treatment with ATRA, cells were fixed and stained with a monoclonal antibody against cytochrome *c* (top, left and middle) or with a normal mouse IgG (top, right). The cell nuclei were stained with 4,6-diamidino-2-phenylindole (DAPI) (bottom). The arrows indicate apoptotic cells with condensed and fragmented nuclei. (**c**) Expression levels of p53 and its direct target gene products in response to ATRA. At the indicated time periods after the treatment with ATRA, whole-cell lysates were prepared, and subjected to immunoblotting with antibodies against p53, Bax, Puma, $p21^{WAF1}$ and actin. Immunoblotting for actin is shown as a control for protein loading (bottom).

Figure 1 Effects of all-*trans* retinoic acid (ATRA) on cell proliferation of LA-N-5, RTBM1, CHP134 and NB-39-nu neuroblastoma-derived cell lines. (**a**) Growth curves of the indicated neuroblastoma cell lines in the presence or absence of ATRA. Cells were grown in the standard culture medium, and treated with 5 μM of ATRA. At the indicated time points after the treatment with ATRA, cells were trypsinized, harvested and number of viable cells was counted in triplicate. (**b**) ATRA-induced morphological changes of neuroblastoma cell lines. Cells were exposed to ATRA at a final concentration of 5 μM or left untreated. Six days after the treatment with ATRA, cells were examined by phase-contrast microscopy. (**c** and **d**) ATRA-induced cell death through apoptosis in CHP134 and NB-39-nu cells. Cells were treated with the indicated concentrations of ATRA or left untreated, and incubated for up to 6 days. At the indicated time points after the treatment with ATRA, cells were collected, fixed and stained with propidium iodide (PI). The DNA content of the cells was then examined by flow cytometry (**c**). The number of cells with sub-G1 DNA content was counted in triplicate (**d**).

that cytochrome *c* release from mitochondria might play an important role in ATRA-induced apoptotic cell death in neuroblastoma cells.

As the neuroblastoma cell lines that we examined carry wild-type p53 (data not shown), we investigated whether p53 could contribute to the ATRA-mediated apoptotic cell death. For this purpose, whole-cell lysates prepared from the indicated neuroblastoma cells exposed to 5 μM of ATRA for 0, 2, 4 and 6 days were processed for immunoblotting with the indicated antibodies. As shown in Figure 2c, the amounts of p53 remained unchanged or slightly decreased after ATRA treatment. In accordance with these results, ATRA had undetectable effects on the expression levels of p53-responsible Bax, Puma and $p21^{WAF1}$, which are implicated in the p53-dependent apoptosis and/or cell cycle arrest (Culmsee and Mattson, 2005). In addition, ATRA failed to induce the phosphorylation of p53 at Ser-15 (data not shown). Thus, it is likely that ATRA-mediated apoptotic cell death in neuroblastoma cells may be regulated in a p53-independent manner.

Differential expression of antiapoptotic Bcl-2 in neuroblastoma cells

To investigate the regulatory mechanisms of apoptotic response to ATRA in neuroblastoma cells, we examined the expression levels of Bcl-2 family proteins, which directly control the mitochondrial pathway of apoptosis. It is worth noting that antiapoptotic Bcl-2 was constitutively expressed at high levels in LA-N-5 as well as RTBM1 cells, whereas CHP134 and NB-39-nu cells expressed Bcl-2 at extremely low levels (Figure 3a). Antiapoptotic Bcl-x_L was expressed at low levels in all cell lines examined. In accordance with the previous observations showing that proapoptotic Bim and Bmf are highly expressed in neuronal cells (Puthalakath *et al.*, 2001; Okuno *et al.*, 2004; Shi *et al.*, 2004), Bim and Bmf were expressed at high levels in all of the cell lines that we examined, but their expression levels remained unchanged in the presence of ATRA.

To determine whether Bcl-2 could contribute to the acquisition of the ATRA-resistant phenotype of neuroblastoma cells, CHP134 cells were transfected with the expression plasmid for Bcl-2 or with the empty plasmid, and their sensitivity to ATRA was examined by flow cytometry. As shown in Figure 3b, Bcl-2 was successfully overexpressed in CHP134 cells as examined by immunoblotting. Interestingly, enforced expression of Bcl-2 inhibited the ATRA-mediated proteolytic cleavage of caspase-3. Consistent with these results, flow cytometric analysis demonstrated that ectopic expression of Bcl-2 significantly reduced the number of cells with sub-G1 DNA content induced by ATRA treatment (Figure 3c and d), suggesting that Bcl-2 might play a critical role in the regulation of apoptotic cell death in neuroblastoma cells.

To further confirm this possibility, we examined the effects of the Bcl-2 inhibitor HA14-1 (Wang *et al.*, 2000) on the ATRA-mediated apoptotic response of neuroblastoma cells. RTBM1 cells were treated with 5 μM of ATRA or left untreated for 6 days, and then incubated in the presence or absence of HA14-1 (15, 30 or 50 μM) for 3 h. Phase-contrast microscopic analysis showed that the incubation with ATRA followed by HA14-1 treatment significantly enhanced the apoptotic response of RTBM1 cells, whereas HA14-1 treatment alone increased the number of apoptotic cells to a lesser degree (Figure 4a). Similar results were also obtained by flow cytometric analysis (Figure 4b and c). To examine whether the ATRA-mediated apoptosis in RTBM1 cells induced by HA14-1 treatment could be associated with the activation of the mitochondria-dependent apoptotic pathway, we performed immunoblot analysis. As shown in Figure 4d, HA14-1 treatment at 30 μM or less did not promote the activation of caspase-9 and caspase-3, whereas a small amount of the cleaved caspase-9 and caspase-3 were detectable in RTBM1 cells exposed to 50 μM of HA14-1 alone. Intriguingly, pre-treatment of RTBM1 cells with ATRA enhanced the proteolytic cleavage of caspase-9 and caspase-3 induced by HA14-1 at a final concentration of 50 μM.

To ask whether Bcl-2 could play an important role in ATRA-mediated apoptotic response in primary neuroblastomas, 10 sporadically found neuroblastomas were subjected to both primary culture and reverse transcriptase–polymerase chain reaction (RT-PCR) analysis for *bcl-2*. In five cases, ATRA treatment induced strong outgrowth of neurites as compared with control culture (Figure 5a, left). In the other three cases, ATRA had undetectable effects (data not shown). It is worth noting that many cells underwent cell death after ATRA treatment in the remaining two cases (Figure 5a, right). We also examined the expression levels of *bcl-2* of these 10 primary neuroblastoma samples and four neuroblastoma-derived cell lines by RT–PCR. LA-N-5 and RTBM1 cells abundantly expressed *bcl-2*, whereas CHP134 and NB-39-nu did not (Figure 5b), which was consistent with immunoblotting as shown in Figure 3a. Of particular interest, RT–PCR analysis revealed that two primary cases that underwent cell death in response to ATRA (N-9 and N-10) expressed *bcl-2* at undetectable levels (Figure 5c). In a sharp contrast, the expression of *bcl-2* was detected in the remaining cases, except N-3. Taken together, our present results strongly suggest that Bcl-2 is a key regulator for ATRA-mediated apoptotic cell death in neuroblastoma cells.

Discussion

Retinoic acid is one of the potent antitumor agents that has been used successfully to treat certain human tumors including neuroblastomas (Freemantle *et al.*, 2003). Indeed, neuroblastoma patients treated with RA have increased survival rate without severe side effects (Villablanca *et al.*, 1995; Matthay *et al.*, 1999). Accumulating evidences suggest that RA plays an important role in the regulation of neuroblastoma apoptosis as well as differentiation (Melino *et al.*,

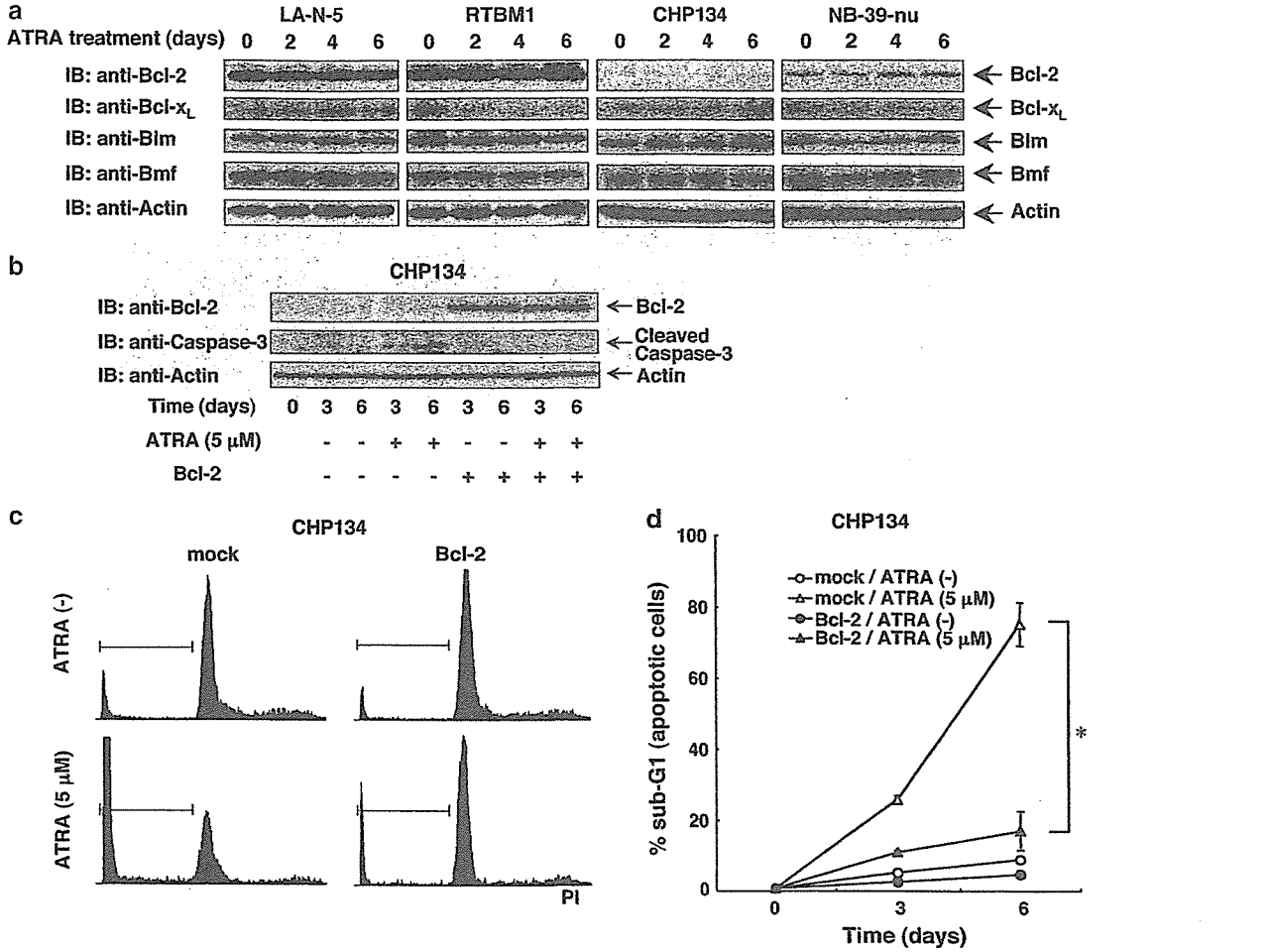

Figure 3 Differential expression of antiapoptotic Bcl-2 protein. (**a**) The indicated neuroblastoma cell lines were cultured in standard culture medium containing all-*trans* retinoic acid (ATRA) at a final concentration of 5 μM. At the indicated time points after the treatment with ATRA, whole-cell lysates were prepared, and analysed by immunoblotting with the antibodies against the indicated Bcl-2 family proteins. Actin expression was examined as a loading control (bottom). (**b**) Overexpression of Bcl-2. CHP134 cells were transiently transfected with the expression plasmid for Bcl-2 or with the empty plasmid. Twelve hours after the transfection, cells were treated with or without 5 μM ATRA, and incubated for additional 3 or 6 days. Whole-cell lysates were prepared, and the expression levels of Bcl-2 (top) and the amounts of the cleaved caspase-3 (middle) were examined by immunoblotting. Actin is shown as a control for protein loading (bottom). (**c** and **d**) Flow cytometry. CHP134 cells were transiently transfected as described in (**b**). At the indicated time periods after the treatment with ATRA, cells were collected, fixed and stained with PI. The DNA content of the cells was examined by flow cytometry. Representative results on day 6 are shown in (**c**). The number of cells with sub-G1 DNA content was counted in triplicate (**d**). *$P<0.01$.

1997; van Noesel and Versteeg, 2004). However, certain neuroblastomas display an RA-resistant phenotype (Reynolds and Lemons, 2001). To further improve the therapeutic effects of RA on neuroblastomas, it is necessary to clarify the detailed molecular mechanisms underlying the RA-mediated neuroblastoma differentiation and/or apoptosis. In the present study, we have found that ATRA causes growth suppression and subsequent neuronal differentiation in human neuroblastoma-derived LA-N-5, RTBM1, CHP134 and NB-39-nu cells to various degrees. Among them, CHP134 and NB-39-nu cells, which express antiapoptotic Bcl-2 at extremely low levels, underwent p53-independent apoptotic cell death in response to ATRA. In contrast, LA-N-5 and RTBM1 cells abundantly expressed Bcl-2, and we did not detect apoptotic cell death upon ATRA treatment. Enforced expression of Bcl-2 in CHP134 cells inhibited the ATRA-mediated apoptosis, and HA14-1-mediated inhibition of the endogenous Bcl-2 in RTBM1 cells enhanced the ATRA-dependent apoptotic cell death. Moreover, studies using primary neuroblastoma tissues showed that ATRA had toxic effect on two out of 10 primary cultures, and these ATRA-sensitive tumors did not express *bcl-2*. Thus, it is likely that antiapoptotic Bcl-2 plays a crucial role in the regulation of the ATRA-mediated apoptotic response in neuroblastomas.

Our present study revealed that neuroblastoma cells can be divided into two groups with respect to the ATRA-induced apoptotic response. CHP134 and NB-39-nu cells underwent apoptotic cell death in response to ATRA, whereas LA-N-5 and RTBM1 cells did not. Consistent with the mitochondria-dependent intrinsic apoptotic pathway of caspase activation (Degterev

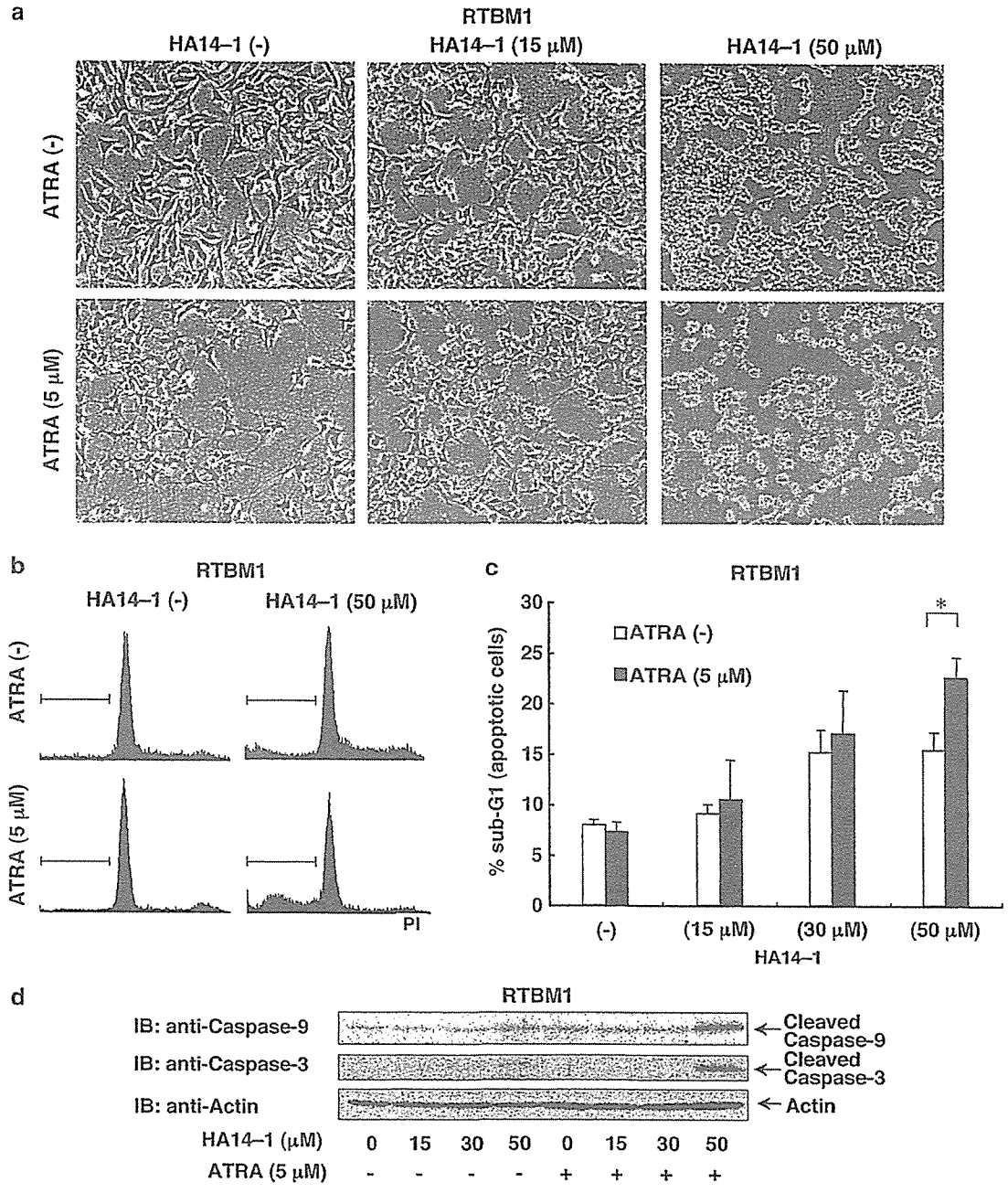

Figure 4 Bcl-2 inhibitor HA14-1 induces apoptosis of all-*trans* retinoic acid (ATRA)-treated RTBM1 cells. (**a**) Morphological changes after HA14-1 treatment of RTBM1 cells. RTBM1 cells were cultured with or without 5 μM ATRA for 6 days in advance, and then treated with HA14-1, a specific inhibitor of Bcl-2, at the indicated concentrations in standard medium for 3 h. Cells were examined by phase-contrast microscopy and photographed after the treatment. (**b** and **c**) FACS analysis. RTBM1 cells were treated with ATRA and HA14-1 as described in (**a**). Cells were collected, fixed and stained with PI. The DNA content of the cells was examined by flow cytometry and representative results are shown in (**b**). The number of cells with sub-G1 DNA content was counted in triplicate (**c**). $^*P<0.05$. (**d**) Immunoblotting. Whole-cell lysates of RTBM1 treated with ATRA and HA14-1 were prepared to examine the amounts of cleaved caspase-9 and caspase-3. Actin is shown as a loading control.

et al., 2003), ATRA treatment in CHP134 cells caused a cytoplasmic release of the mitochondrial inter-membrane protein cytochrome *c*, and a sequential proteolytic cleavage of caspase-9, caspase-3 and its physiological substrate PARP. Similar results were obtained in NB-39-nu cells. Our previous observation also demonstrated that activation and nuclear translocation of caspases were associated with prognosis of primary neuroblastomas (Nakagawara *et al.*, 1997). Therefore, the molecular mechanism(s) of RA-induced activation of caspases in neuroblastoma cells needs to be clarified.

In response to a variety of apoptotic stimuli, p53 is induced to be stabilized and subsequently transactivates a number of proapoptotic genes that encode Bcl-2

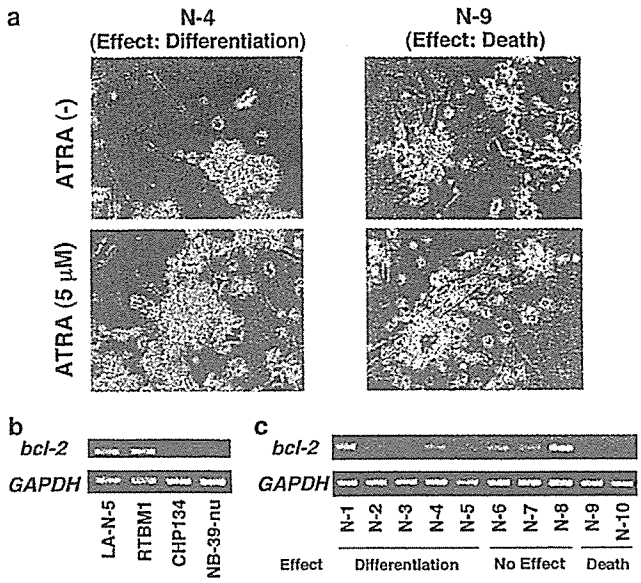

Figure 5 Primary culture and *bcl-2* expression of sporadic neuroblastomas. (a) Primary tumor cells prepared from 10 sporadically found neuroblastoma tissues were cultured with or without 5 μM of ATRA. After 4 days, cells were examined by phase-contrast microscope, and morphological changes of two representative cases are shown. (b and c) RT–PCR analysis. Total RNA was purified from the indicated neuroblastoma cell lines (b) and fresh-frozen tissues of primary neuroblastomas (c), and subjected to RT–PCR using specific primers for *bcl-2*. N-1 to N-10 indicates the case numbers, and the effects of ATRA on primary cultures are described at the bottom of this panel. Glyceraldehyde-3-phosphate dehydrogenase (*GAPDH*) expression is shown as an internal control.

family proteins including Bax (Culmsee and Mattson, 2005). It has been well documented that Bax acts on the mitochondria to induce mitochondrial permeability transition, and thereby regulating the cytoplasmic release of cytochrome *c* (Antonsson, 2001). Neuroblastoma cell lines that we examined in this study carry wild-type p53. Under our experimental conditions, however, we could not detect the ATRA-mediated upregulation of the endogenous p53 as well as Bax. Similarly, the p53-responsible $p21^{WAF1}$ and proapoptotic Puma were not accumulated in response to ATRA. As described (Nikolaev *et al.*, 2003), p53 might not be functional in neuroblastoma cells due to its abnormal cytoplasmic retention. Consistent with this notion, p53 was predominantly expressed in the cytoplasm of neuroblastoma cells examined in this study (data not shown). We have previously shown that cytoplasmic p53 is translocated into the nucleus of CHP134 cells in response to ATRA (Takada *et al.*, 2001); however, our present results suggest that translocated p53 was not functional. Indeed, it is reported that p53 in neuroblastoma cells is not functional even after its enforced translocation into the nucleus (Ostermeyer *et al.*, 1996). Thus, it is likely that the ATRA-mediated apoptotic cell death in neuroblastoma cells is regulated in a p53-independent manner.

Among other regulators of mitochondrial pathway of apoptosis, Bcl-2 family proteins are critical determinants of mitochondrial membrane potential, which controls the cytoplasmic release of cytochrome *c* from mitochondria and thereby regulating apoptotic cell death (Cory *et al.*, 2003). They are divided into two subfamilies based on their biological roles. Antiapoptotic subfamily includes Bcl-2 and Bcl-x_L and proapoptotic subfamily includes Bax, Bim and Bmf. The balance between these two groups determines the fate of cells. Antiapoptotic Bcl-2 is one of the most important members that inhibits the mitochondria-dependent apoptotic pathway triggered by diverse cytotoxic agents through blocking mitochondrial permeability transition. Indeed, the upregulation of Bcl-2 was associated with the drug-resistant phenotype of certain human tumors (Dole *et al.*, 1994; Lombet *et al.*, 2001). Most intriguingly, our expression studies revealed that antiapoptotic Bcl-2 was constitutively overexpressed in LA-N-5 and RTBM1 cells, whereas its expression levels were extremely low in CHP134 and NB-39-nu cells. In response to ATRA, Bcl-2 was slightly induced to be accumulated in NB-39-nu cells; however, it was maintained at extremely low levels in CHP134 cells. Furthermore, two primary neuroblastomas on which ATRA had toxic effect in primary culture did not express *bcl-2*, similar to CHP134 and NB-39-nu cells. Interestingly, ATRA induced differentiation in five cases and had undetectable effects on three cases, but cell death was induced in two cases. Considering that RA treatment contributed to survival of 17% of patients with aggressive neuroblastomas (Matthay *et al.*, 1999), our present results using primary neuroblastomas seem to be reliable. Taken together, it is likely that ATRA potentially have toxic effect on certain neuroblastoma cells (both primary cells and cell lines) that express little Bcl-2. Our current results also revealed that enforced expression of Bcl-2 in CHP134 cells inhibited the ATRA-mediated apoptosis in association with the activation of caspase-3. Furthermore, ATRA treatment of RTBM1 cells followed by HA14-1 exposure underwent apoptotic cell death through mitochondrial pathway. These observations also support the importance of Bcl-2 in the regulation of apoptotic response of neuroblastoma cells to RA.

Although it is still unclear whether the expression levels of Bcl-2 could be correlated with the prognosis of neuroblastoma patients (Romani and Lu, 1994; Gallo *et al.*, 2003; Abel *et al.*, 2005), it is possible that Bcl-2 plays a key role at least in part in the regulation of ATRA-mediated apoptotic cell death in neuroblastoma cells. In this connection, the antisense RNA-mediated knockdown of the endogeneous Bcl-2 has been employed to treat certain tumors (Kim *et al.*, 2004). Recently, a novel Bcl-2 inhibitor that has an antitumor effect on solid tumors has been developed (Oltersdorf *et al.*, 2005). Based on our present findings, the combination of RA with Bcl-2-specific inhibitor might provide a novel therapeutic strategy for the treatment of neuroblastomas, instead of the classical chemotherapy that frequently has multi-organ side effects.

Materials and methods

Cell lines and transfection

Human neuroblastoma-derived cell lines, including LA-N-5, RTBM1, CHP134 and NB-39-nu, were maintained in RPMI 1640 medium supplemented with 10% heat-inactivated fetal bovine serum, penicillin (50 U/ml) and streptomycin (50 μg/ml) at 37°C in a humidified atmosphere of 5% CO_2 in the air. For transfection, CHP134 cells were transfected with the expression plasmid encoding human Bcl-2 or with the empty plasmid by electroporation using a Nucleofector (Amaxa Biosystems, Koeln, Germany) according to the manufacturer's protocol.

Reagents

All-*trans* retinoic acid was purchased from Sigma (St Louis, MO, USA) dissolved in dimethylsulfoxisde (DMSO) at a final concentration of 5 mM, and kept at −80°C. Bcl-2 inhibitor HA14-1 was purchased from Sigma, dissolved in DMSO as a 10 mM stock solution and stored at −20°C. All reagents were of the highest quality available.

Proliferation assay

LA-N-5 and RTBM1 cells were plated in triplicate at a density of 1×10^5 per well in 12-well culture plates. CHP134 and NB-39-nu cells were seeded in triplicate at a density of 1×10^4 in 12-well plates. Twelve hours after seeding the cells, cells were treated with ATRA at a final concentration of 5 μM or left untreated, and medium was replaced every 2 days. At the indicated time points after the treatment with ATRA, cells were trypsinized and number of viable cells was directly scored by using the hemocytometer.

Flow cytometric analysis

Cells were exposed to the indicated concentration of ATRA. At the indicated time points after the treatment with ATRA, cells were collected by brief centrifugation, and fixed with 70% ethanol at −20°C. The cells were washed with phosphate-buffered saline (PBS), resuspended in phosphate-citrate buffer (4 mM citric acid, 200 mM Na_2HPO_4) and kept at room temperature for 15 min. The cells were then centrifuged and resuspended in a solution containing 40 μg/ml of propidium iodide and 0.05% RNase A, and incubated in the dark for 30 min. Before performing flow cytometric analysis, cells were filtered through a 40-μm nylon mesh. DNA content was analysed by FACScan flow cytometer (Becton Dickinson, Oxford, UK).

Immunoblot analysis

Cells were washed twice with ice-cold PBS, lysed in a sodium dodecyl sulfate (SDS)-sample buffer containing 10% glycerol, 5% β-mercaptoethanol, 2.3% SDS and 62.5 mM Tris-HCl, pH 6.8, and then boiled for 3 min. The protein concentrations were determined using Bio-Rad protein assay dye reagent (Bio-Rad Laboratories, Hercules, CA, USA). Bovine serum albumin (BSA) was used as a standard. Aliquots (20 μg) of whole-cell lysates were separated by SDS–polyacrylamide gel electrophoresis and electrophoretically transferred onto polyvinylidene difluoride membranes (Immobilon-P, Millipore, Bedford, MA, USA). The membranes were blocked with 0.3% non-fat milk in Tris-buffered saline containing 0.1% Tween-20 and incubated with appropriate primary antibodies at room temperature for 1 h followed by incubation with the horseradish peroxidase-conjugated secondary antibodies (Cell Signaling Technology Inc., Beverly, MA, USA). Immunoreactive bands were visualized by using ECL system (Amersham Biosciences, Uppsala, Sweden). The primary antibodies used in this study were as follows: polyclonal anti-caspase-12 (Cell Signalling Technology Inc.), polyclonal anti-caspase-3 (Calbiochem, San Diego, CA, USA), polyclonal anti-PARP (Cell Signaling Technology Inc.), polyclonal anti-PUMA (ab9643; Abcam, Cambridge, UK), polyclonal anti-$p21^{WAF1}$ (H-164; Santa Cruz Biotechnology), polyclonal anti-Bim (Cell Signaling Technology Inc.), polyclonal anti-Bmf (Cell Signaling Technology Inc.), polyclonal anti-actin (20-33; Sigma), monoclonal anti-caspase-8 (5F7; Medical & Biological Laboratories, Nagoya, Japan), monoclonal anti-caspase-9 (5B4; Medical & Biological Laboratories), monoclonal anti-p53 (DO-1; Oncogene Research Products, Cambridge, MA, USA), monoclonal anti-Bax (6A7; eBioscience, San Diego, CA, USA), monoclonal anti-Bcl-2 (100; Santa Cruz Biotechnology); and monoclonal anti-Bcl-x_L (H-5; Santa Cruz Biotechnology) antibodies.

Immunofluorescent staining

CHP134 cells were grown on coverslips in standard culture medium in the presence or absence of 5 μM of ATRA for 4 days. Cells were washed with ice-cold PBS, fixed with 3.7% formaldehyde in PBS for 30 min, permeabilized with 0.2% Triton X-100 in PBS for 5 min and then blocked with 3% BSA in PBS for 1 h at room temperature. After blocking, cells were incubated with a monoclonal antibody against cytochrome *c* (6H2.B4; BD PharMingen, San Jose, CA, USA) or with a normal mouse IgG for 1 h at room temperature, followed by the incubation with fluorescein isothiocyanate-conjugated secondary antibody against mouse IgG (Santa Cruz Biotechnology). The cell nuclei were stained with DAPI. The coverslips were mounted onto glass slides, and the stained cells were examined by using a confocal laser scanning microscope (Olympus).

Primary culture

RPMI 1640 medium supplemented with 10% heat-inactivated fetal bovine serum, penicillin (50 U/ml), streptomycin (50 μg/ml) and 100 μg/ml of OPI (Sigma) was used as a standard medium for primary culture. Primary tumor cells were prepared from fresh human neuroblastoma tissues by a standard method. A total of 5×10^5 cells of each sample were resuspended in 1 ml of the standard medium, and seeded on 24-well tissue culture plates precoated with collagen. The cells were treated with or without ATRA at a final concentration of 5 μM for at least 2 weeks. The effects of ATRA on the growth and neurite extension of primary neuroblastoma cells were examined by phase-contrast microscope.

RNA extraction and RT–PCR

Total RNA was prepared from fresh-frozen tissues of primary neuroblastomas or cultured cells by using RNeasy Mini Kit (Qiagen, Valencia, CA, USA). Total RNA (2 μg) was reverse transcribed by using random primers and SuperScript II reverse transcriptase (Invitrogen, Carlsbad, CA, USA). The resultant cDNA was subjected to PCR-based amplification. The oligonucleotide primers used in this study were as follows: *bcl-2*, 5′-GAGGATTGTGGCCTTCTTTG-3′ (forward) and 5′-ACAGTTCCACAAAGGCATCC-3′ (reverse), and glyceraldehyde-3-phosphate dehydrogenase (*GAPDH*), 5′-ACCTGACCTGCCGTCTAGAA-3′ (forward) and 5′-TCCACCACCCTGTTGCTGTA-3′ (reverse). PCR products were electrophoretically separated on 1% neutral agarose gels and visualized by ethidium bromide staining.

Acknowledgements

We are grateful to the hospitals and institutions that provided us with surgical specimens. We thank Hideki Yamamoto and Atsushi Kawasaki for valuable discussions, and Yuki Nakamura for excellent technical assistance. This work was supported in part by a Grant-in-Aid from the Ministry of Health, Labour and Welfare for Third Term Comprehensive Control Research for Cancer, and a Grant-in-Aid for Scientific Research on Priority Areas and a Grant-in-Aid for Scientific Research (C) from the Ministry of Education, Culture, Sports, Science and Technology, Japan.

References

Abel F, Sjoberg RM, Nilsson S, Kogner P, Martinsson T. (2005). *Eur J Cancer* **41**: 635–646.
Antonsson B. (2001). *Cell Tissue Res* **306**: 347–361.
Balmer JE, Blomhoff R. (2002). *J Lipid Res* **43**: 1773–1808.
Brodeur GM. (2003). *Nat Rev Cancer* **3**: 203–216.
Brodeur GM, Nakagawara A. (1992). *Am J Pediatr Hematol Oncol* **14**: 111–116.
Cory S, Huang DC, Adams JM. (2003). *Oncogene* **22**: 8590–8607.
Culmsee C, Mattson MP. (2005). *Biochem Biophys Res Commun* **331**: 761–777.
Degterev A, Boyce M, Yuan J. (2003). *Oncogene* **22**: 8543–8567.
Dole M, Nunez G, Merchant AK, Maybaum J, Rode CK, Bloch CA *et al.* (1994). *Cancer Res* **54**: 3253–3259.
Encinas M, Iglesias M, Llecha N, Comella JX. (1999). *J Neurochem* **73**: 1409–1421.
Freemantle SJ, Spinella MJ, Dmitrovsky E. (2003). *Oncogene* **22**: 7305–7315.
Gallo G, Giarnieri E, Bosco S, Cappelli C, Alderisio M, Giovagnoli MR *et al.* (2003). *Anticancer Res* **23**: 777–784.
Kim R, Emi M, Tanabe K, Toge T. (2004). *Cancer* **101**: 2491–2502.
Lee MH, Nikolic M, Baptista CA, Lai E, Tsai LH, Massague J. (1996). *Proc Natl Acad Sci USA* **93**: 3259–3263.
Lippman SM, Lotan R. (2000). *J Nutr* **130**: 479S–482S.
Lombet A, Zujovic V, Kandouz M, Billardon C, Carvajal-Gonzalez S, Gompel A *et al.* (2001). *Eur J Biochem* **268**: 1352–1362.
Lopez-Carballo G, Moreno L, Masia S, Perez P, Barettino D. (2002). *J Biol Chem* **277**: 25297–25304.
Maden M. (2001). *Int Rev Cytol* **209**: 1–77.
Matthay KK, Villablanca JG, Seeger RC, Stram DO, Harris RE, Ramsay NK *et al.* (1999). *N Engl J Med* **341**: 1165–1173.
McCaffery PJ, Adams J, Maden M, Rosa-Molinar E. (2003). *Eur J Neurosci* **18**: 457–472.
Melino G, Thiele CJ, Knight RA, Piacentini M. (1997). *J Neurooncol* **31**: 65–83.
Morishima N, Nakanishi K, Takenouchi H, Shibata T, Yasuhiko Y. (2002). *J Biol Chem* **277**: 34287–34294.
Nagai J, Yazawa T, Okudela K, Kigasawa H, Kitamura H, Osaka H. (2004). *Cancer Res* **64**: 7910–7917.
Nakagawa T, Zhu H, Morishima N, Li E, Xu J, Yankner BA *et al.* (2000). *Nature* **403**: 98–103.
Nakagawara A. (1998). *Hum Cell* **11**: 115–124.
Nakagawara A, Arima-Nakagawara M, Scavarda NJ, Azar CG, Cantor AB, Brodeur GM. (1993). *N Engl J Med* **328**: 847–854.
Nakagawara A, Azar CG, Scavarda NJ, Brodeur GM. (1994). *Mol Cell Biol* **14**: 759–767.
Nakagawara A, Nakamura Y, Ikeda H, Hiwasa T, Kuida K, Su MS *et al.* (1997). *Cancer Res* **57**: 4578–4584.
Nakamura Y, Ozaki T, Koseki H, Nakagawara A, Sakiyama S. (2003). *Biochem Biophys Res Commun* **307**: 206–213.
Nikolaev AY, Li M, Puskas N, Qin J, Gu W. (2003). *Cell* **112**: 29–40.
Okuno S, Saito A, Hayashi T, Chan PH. (2004). *J Neurosci* **24**: 7879–7887.
Oltersdorf T, Elmore SW, Shoemaker AR, Armstrong RC, Augeri DJ, Belli BA *et al.* (2005). *Nature* **435**: 677–681.
Ostermeyer AG, Runko E, Winkfield B, Ahn B, Moll UM. (1996). *Proc Natl Acad Sci USA* **93**: 15190–15194.
Piacentini M, Annicchiarico-Petruzzelli M, Oliverio S, Piredda L, Biedler JL, Melino G. (1992). *Int J Cancer* **52**: 271–278.
Puthalakath H, Villunger A, O'Reilly LA, Beaumont JG, Coultas L, Cheney RE *et al.* (2001). *Science* **293**: 1829–1832.
Reynolds CP, Lemons RS. (2001). *Hematol Oncol Clin N Am* **15**: 867–910.
Romani P, Lu QL. (1994). *J Pathol* **172**: 273–278.
Schor NF. (1999). *J Neurooncol* **41**: 159–166.
Shi L, Gong S, Yuan Z, Ma C, Liu Y, Wang C *et al.* (2004). *Neurosci Lett* **375**: 7–12.
Takada N, Isogai E, Kawamoto T, Nakanishi H, Todo S, Nakagawara A. (2001). *Med Pediatr Oncol* **36**: 122–126.
Teitz T, Wei T, Valentine MB, Vanin EF, Grenet J, Valentine VA *et al.* (2000). *Nat Med* **6**: 529–535.
Thiele CJ, Reynolds CP, Israel MA. (1985). *Nature* **313**: 404–406.
Van Noesel MM, Van Bezouw S, Voute PA, Herman JG, Pieters R, Versteeg R. (2003). *Genes Chromosomes Cancer* **38**: 226–233.
Van Noesel MM, Versteeg R. (2004). *Gene* **325**: 1–15.
Villablanca JG, Khan AA, Avramis VI, Seeger RC, Matthay KK, Ramsay NK *et al.* (1995). *J Clin Oncol* **13**: 894–901.
Wang JL, Liu D, Zhang ZJ, Shan S, Han X, Srinivasula SM *et al.* (2000). *Proc Natl Acad Sci USA* **97**: 7124–7129.

Aberrant methylation of *RASGRF2* and *RASSF1A* in human non-small cell lung cancer

HONG CHEN[1,3], MAKOTO SUZUKI[1,4], YOHKO NAKAMURA[2], MIKI OHIRA[2], SOICHIRO ANDO[1], TOMOHIKO IIDA[1], TAKAHIRO NAKAJIMA[1], AKIRA NAKAGAWARA[2] and HIDEKI KIMURA[1]

Divisions of [1]Thoracic Diseases and [2]Biochemistry, Chiba Cancer Center, 666-2 Nitona, Chuoh-ku, Chiba 260-8717; [3]Department of Pulmonary Disease, The First Affiliated Hospital, Chongqing University of Medical Sciences, 1 Youyi Road, Yuzhong District, Chongqing, 400016, P.R. China

Received February 9, 2005; Accepted April 16, 2005

Abstract. Aberrant methylation of promoter CpG that causes silencing of tumor suppressor genes (TSGs) may play a key role in the carcinogenesis of many cancer types. *RASSF1A*, regarded as a TSG, has been extensively studied in lung cancer and other malignant tumors, whereas *RASGRF2* has only been reported to possibly play a role in the pathogenesis of pancreatic cancer cell lines. The aims of our study were to i) determine the methylation profile of *RASGRF2* and ii) compare the methylation profiles of *RASGRF2* with *RASSF1A* in lung cancer. We examined *RASGRF2* expression by reverse transcription PCR and aberrant methylation of *RASGRF2* by methylation-specific PCR in lung cancer cell lines. Loss of *RASGRF2* expression was presented in 36% lung cancer cell lines while aberrant methylation of *RASGRF2* was present in 30% (3/10) non-small cell lung cancer (NSCLC) cell lines and in 25% (1/4) small cell lung cancer (SCLC) cell lines. The concordance between loss of expression and aberrant methylation of *RASGRF2* was 86% (12/14). *RASGRF2* expression was restored after treatment with the demethylating agent, 5-aza-2'-deoxycytidine in all four cell lines tested that downregulated *RASGRF2* expression. Among primary NSCLC, *RASGRF2* and *RASSF1A* methylation was observed in 34% (39/114) and 39% (44/114) of cases respectively, while it was observed in only 7% (4/57) and none of the corresponding non-malignant lung tissue. There is no correlation between *RASGRF2* and *RASSF1A* methyl-ation status. Both *RASGRF2* and *RASSF1A* methylation did not associate with clinical characteristics. Frequent methylation and silencing of *RASGRF2* in tumor cells may play an important role, different from that of *RASSF1A*, in the carcinogenesis of NSCLC.

Correspondence to: Dr Makoto Suzuki, [4]*Present address*: Department of Thoracic Surgery, Graduate School of Medicine, Chiba University, 1-8-1 Inohana, Chuoh-ku, Chiba 260-8677, Japan
E-mail: makotosuzuki@hotmail.co.jp

Key words: RASGRF2, RASSF1A, methylation, lung cancer

Introduction

Aberrant methylation of promoter CpG that causes silencing of tumor suppressor genes (TSGs) may play a key role in the carcinogenesis of many cancer types. Recent advances in molecular genetics have showed that multiple TSGs are involved in human lung cancer pathogenesis (1).

Ras association domain family 1A (*RASSF1A*) is located within a 120-kb region of chromosome 3p21, a region that is epigenetically inactivated at high frequency in non-small cell lung cancer (NSCLC) (2). Further studies reveal that, in addition to loss of heterozygosity (LOH), promoter hypermethylation of *RASSF1A* is another mechanism of this gene's loss of expression (3-5). It has been shown that *RASSF1A* bind to the Ras-GTP binding protein, Nore1, which is consistent with the role of a negative effector of Ras oncoprotein (6). *RASSF1A* could induce cell cycle arrest by engaging the RB cell cycle checkpoint. Inhibition of cyclin D1 by *RASSF1A* occurs post-transcriptionally and is likely at the level of translational control. These results strongly suggest that *RASSF1A* is an important human tumor suppressor protein acting at the level of G(1)/S-phase cell cycle progression (7).

Ras protein-specific guanine nucleotide-releasing factor 2 (*RASGRF2*) was originally found by Anborgh *et al* (8); who, using a yeast 2-hybrid screen of a brain cDNA library with the Dbl homology (DH) domain of RASGRF1 as bait, followed by 5-prime and 3-prime RACE, isolated a full-length cDNA encoding *RASGRF2*. *RASGRF2* is involved in H-Ras signaling (9) and abundantly expressed in a variety of tissue, such as brain, heart and lung (8). However, its expression is decreased in rat mammary carcinomas (10). Recently, it was reported that *RASGRF2* was abundantly expressed in at least one of two ductal epithelial cell lines, but there was loss of expression due to promoter methylation in pancreatic cancer cell lines, using high-throughput microarray analysis (11). Among the 12 genes silenced by methylation of 5' regions, *RASGRF2* was methylated at about 17%, which is higher than a few other genes. This gene is located at a region of chromosome

Table I. Clinical characteristics and *RASGRF2* and *RASSF1A* methylation of lung cancer patients.

Clinical factors	No. of cases	No. of *RASGRF2* methylation (%)	p-value[a]	No. of *RASSF1A* methylation (%)	p-value[a]
Gender					
Male	65	25 (38)	0.32	24 (37)	0.70
Female	49	14 (29)		20 (41)	
Age					
≤66[b]	58	20 (34)	>0.99	19 (33)	0.25
>66	56	19 (34)		25 (45)	
Smoke					
Never	42	12 (29)	0.41	18 (43)	0.55
Smoker	72	27 (38)		26 (36)	
Histology					
Adenocarcinoma	85	28 (38)		36 (42)	
Squamous cell carcinoma	27	11 (41)	0.30[c]	7 (26)	0.10
Others (ad-sq, large)	2	0		1 (50)	
PT					
T1	50	15 (30)	0.26	19 (38)	0.53
T2, 3, 4	64	24 (38)		25 (39)	
pN					
N0	68	25 (37)	0.31	24 (35)	0.86
N1, 2, 3	46	14 (30)		20 (43)	
pStage					
I	50	18 (36)	0.71	19 (38)	0.53
II, III, IV	64	21 (33)		25 (39)	

[a]Fisher's exact probability test; [b]Divided into two groups by median age; [c]Adenocarcinoma vs. squamous cell carcinoma; Ad-sq, adenosquamous cell carcinoma.

5q13, a locus which frequently shows an allelic imbalance in lung cancer, and was speculated to act as a TSG (12). This prompted us to examine the methylation status of *RASGRF2* in lung cancer.

Imbalance of the Ras signaling pathway is a major hallmark of human cancer. Activated Ras proteins interact with a broad range of effector proteins to induce a diverse series of biological consequences. *RASSF1A* and *RASGRF2*, correlating with Ras-effector, were investigated in this study. We examined the methylation, by methylation-specific PCR (MSP), of *RASSF1A* and *RASGRF2* in lung cancer cell lines, and analyzed the methylation status of primary lung cancer, and correlated them with the clinicopathological features. We examined the mRNA expression of *RASGRF2* by reverse transcription PCR (RT-PCR) and treated those cell lines which showed loss of *RASGRF2* mRNA expression with 5-Aza-CdR.

Materials and methods

Cell lines. Ten non-small cell lung cancer (NSCLC) and 4 small cell lung cancer (SCLC) cell lines were used in this study. These cell lines were established and provided by Dr Adi F. Gazdar. Cell lines were grown in RPMI-1640 medium supplemented with 5% fetal bovine serum and incubated in 5% CO_2 at 37°C. Normal tracheal RNA was obtained from Clontech (Palo Alto, CA), and non-malignant human bronchial epithelial cells (NHBEC) were cultured as reported previously (unpublished data).

Clinical samples. Surgically resected specimens of 114 patients with primary lung cancer and 57 adjacent non-malignant lung tissue samples were obtained from Chiba Cancer Center, Japan, after obtaining Institutional Review Board approval and informed consent. Samples were immediately frozen and stored at -80°C until used. The clinical characteristics of these patients are detailed in Table I.

Methylation assay. Genomic DNA was obtained from lung cancer cell lines, cultured non-malignant cells, primary tumors and adjacent non-malignant tissue, by digestion with 20 mg/ml proteinase K (Life Technologies, Inc.), followed by standard phenol/chloroform (1:1) extraction and ethanol precipitation (13). One μg of genomic DNA was further subjected to bisulfite treatment following the protocol of EZ DNA methylation kit (ZYMO Research, Orange, CA). The modified DNA was used as a template for MSP. DNA methylation patterns in the CpG island of *RASGRF2* were determined by the method of MSP as reported previously (11). Primer sequences of *RASGRF2* for the unmethylated reaction were: 5'-TGGAGAGTGTGTTTTGGTTTTA-3' (sense), and 5'-CCAACCAACAAAAAACACCCC-3' (antisense), which amplify a 117-bp product. Primer sequences of

RASGRF2 for the methylated reaction were: 5'-GGCGGAGAG CGTGTTTC-3' (sense), and 5'-CCGACCGACGAAAAACG-3' (antisense), which amplify a 119-bp product. Primer sequences of *RASSF1A* for the unmethylated reaction were: 5'-GGTT TTGTGAGAGTGTGTTTAG-3' (sense), and 5'-CACTAACA AACACAAACCAAAC-3' (antisense). Primer sequences of *RASSF1A* for the methylated reaction were: 5'-GGGTTTTGCG AGAGCGCG-3' (sense), and 5'-GCTAACAAACGCGAA CCG-3' (antisense). Universal methylated DNA (Chemicon, CA), which was subjected to bisulfite treatment, was used as a positive control for methylated alleles. Negative controls without DNA were included in each assay. Nine μl of each PCR product was loaded on 2% agarose gels stained with ethidium bromide. Results were confirmed by repeating bisulfite treatment and MSP for all samples.

Reverse transcription-PCR for gene expression

RASGRF2. mRNA expression was analyzed by RT-PCR. Total RNA was obtained from cell lines (NHBEC, 10 NSCLC and 4 SCLC), primary tumors and adjacent non-malignant tissue by single-step method. Reverse transcription reaction was performed on 5 μg of total RNA with the SuperScriptII First-Strand Synthesis using oligo (dT) primer system (Life Technologies Inc.), and aliquots of the reaction mixture were used for the subsequent PCR amplification. Expression of ß-actin was used as an internal control to confirm the success of the reverse transcription reaction. The forward PCR amplification primer of *RASGRF2* was 5'-ACATTTTGATTGA GAGGGAAGT-3', and the reverse primer 5'-CGCATTCGTT CTTTGGTTT-3'. The forward PCR amplification primer of ß-actin was 5'-CAACTGGGACGACATGGAGA-3', and the reverse primer 5'-ACGTACATGGTGGGGTGTTG-3'. These primer sequences were identical to the human target genes, as was confirmed by BLAST searches. PCR products were analyzed on 2% agarose gels stained with ethidium bromide. NHBEC and normal trachea were used as normal controls for RT-PCR.

5-aza-2'-deoxycytidine (5-Aza-CdR) treatment. Methylated cell lines that downregulated gene expression were incubated in culture medium with 1 μM of the demethylating agent 5-Aza-CdR (Sigma-Aldrich, St. Louis, MO) for 6 days, with medium changes on days 1, 3 and 5. Cells were harvested and RNA was extracted on day 6.

Statistical analysis. The differences of methylation between two groups were analyzed by using Fisher's exact test. Survival was calculated from the date of initial diagnosis until death or the date of the last follow-up. Survival was analyzed according to the Kaplan-Meier method, and differences in their distribution were evaluated by means of the log-rank test. All p-values are two-sided. The probability value of $p<0.05$ was regarded as statistically significant.

Results

Aberrant methylation of RASSF1A and RASGRF2 in cell lines. Detailed results of aberrant methylation of *RASSF1A* and *RASGRF2* in cell lines are shown in Fig. 1. Aberrant methylation of *RASSF1A* was observed in 79% (11/14) of lung cancer cell lines; in 100% (4/4) of SCLC cell lines and in 70% (7/10) of NSCLC cell lines. Aberrant methylation of both genes was absent in NHBEC. However, aberrant methylation of *RASGRF2* was observed in 29% (4/14) of lung cancer cell lines; in 30% (3/10) of NSCLC cell lines and 25% (1/4) of SCLC cell lines. Only two cell lines (NCI-H524 and NCI-H1299) demonstrated loss of expression and lack of methylation of *RASGRF2*. The concordance between gene expression and methylation of *RASGRF2* was 90% (9/10) in NSCLC cell lines, and 75% (3/4) in SCLC cell lines (overall concordance was 86%). There was no correlation between *RASGRF2* and *RASSF1A* methylation status.

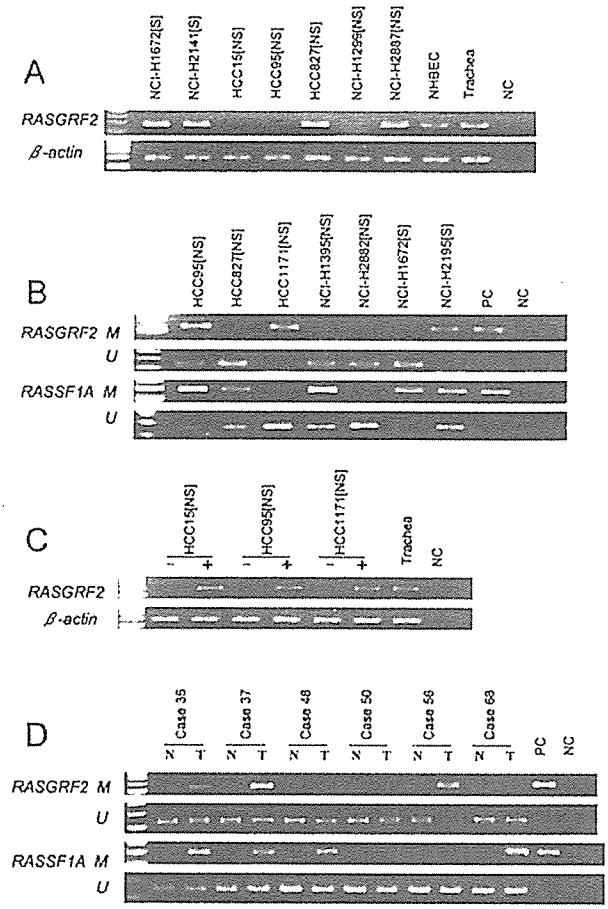

Figure 1. A, Representative examples of RT-PCR assay for *RASGRF2* RNA expression in NSCLC and SCLC cell lines. Expression of ß-actin was used as a control for cDNA normalization. NHBEC and trachea were used as positive control. NC, negative control; NS, NSCLC; S, SCLC. Lanes that do not show a band represent samples with loss of expression. B, Methylation analysis of *RASGRF2* and *RASSF1A* in cell lines. Lane M, amplified product with primers recognizing methylated sequence. Lane U, amplified product with primers recognizing unmethylated sequence. PC, positive control; NC, negative control. C, Re-expression of *RASGRF2* after treatment with 5-Aza-2'-deoxycytidine (5-Aza-CdR). The expression of *RASGRF2* lost in those cell lines can be restored after treatment with 5-Aza-CdR. -, Cell line without 5-Aza-CdR; +, Cell line with 5-Aza-CdR; Trachea was used as positive control. D, Representative examples of methylation analysis of *RASGRF2* and *RASSF1A* in tumor specimens. N, non-malignant lung tissue; T, tumor.

Expression of RASGRF2 in cell lines. *RASGRF2* expression was examined by RT-PCR, representative examples are shown

in Fig. 1. Expression of *RASGRF2* was present in NHBEC and normal trachea. However, loss of *RASGRF2* expression was observed in 36% (5/14) of lung cancer cell lines; in 40% (4/10) of NSCLC cell lines, and 25% (1/4) of SCLC cell lines.

5-Aza-CdR treatment. To confirm that the promoter methylation was responsible for silencing the *RASGRF2* expression, we treated methylated NSCLC cell lines (HCC15, HCC95, HCC1171, NCI-H2195) that showed downregulated *RASGRF2* expression with the demethylating agent 5-Aza-CdR. *RASGRF2* expression was restored after the treatment in all four cell lines tested (Fig. 1).

Aberrant methylation of RASSF1A and RASGRF2 in clinical samples. RASSF1A and *RASGRF2* methylation of primary tumors and corresponding non-malignant tissue is detailed in Table I and representative samples are illustrated in Fig. 1. *RASSF1A* methylation was observed in 39% (44/114) of tumors compared to none in corresponding non-malignant tissue. *RASGRF2* methylation was observed in 34% (39/114) of tumors while only 7% (4/57) was observed in corresponding non-malignant tissue. Methylation of both genes was tumor specific when compared with that of corresponding non-malignant lung tissue ($p<0.0001$). There was no relationship between *RASSF1A* methylation and *RASGRF2* methylation. *RASSF1A* and *RASGRF2* methylation with clinico-pathological features was also examined. There were no significant correlations with gender, age, smoking history (ever vs. never smoker), or histology (adenocarcinoma vs. squamous cell carcinoma), in either gene. *RASSF1A* and *RASGRF2* methylation statuses did not correlate with survival.

Expression of RASGRF2 in clinical samples. We checked 17 clinical samples of *RASGRF2* expression by RT-PCR to confirm the relationship between methylation and expression, representative examples are shown in Fig. 1. Expression of *RASGRF2* was present in non-malignant tissue. However, loss of *RASGRF2* expression was observed in 53% (9/17) of NSCLC tumors. The loss of expression was highly correlated with methylation. The concordance between gene expression and methylation of *RASGRF2* was 65% (11/17).

Discussion

Recently, Hagihara *et al* reported that *RASGRF2* is frequently methylated in pancreatic cancer and thought to be a candidate for a TSG (11). However, there is no report about the role of *RASGRF2* in lung cancer. To understand the role of the *RASGRF2* gene in lung cancer, we examined the expression of *RASGRF2*. *RASGRF2* was expressed in tracheal cells, and cultured airway epithelial cells, whereas lung cancer cell lines had 36% loss of expression. 5-Aza-CdR treatment restored the expression of the gene in RT-PCR-negative cell lines, indicating methylation as a mechanism of transcriptional silencing of the gene. Moreover, methylation of *RASGRF2* was present in 34% of NSCLC with a tumor-specific manner. There are several reports about the correlation between aberrant methylation of TSGs and carcinogenesis of lung cancer (14). *RASGRF2* may be added to the list of TSGs. To our knowledge, this is the first report that demonstrates the methylation of *RASGRF2* promoter in lung cancer.

We found that *RASGRF2* expression was decreased both in lung cancer cell lines and clinical samples, which was the same as in rat mammary carcinomas (10) and in pancreatic cancer cell lines (11). *RASGRF2* has been reported to be involved in H-Ras signaling (9). RAS GTPases cycle between an inactive GDP-bound state and an active GTP-bound state. As guanine-nucleotide exchange factors, *RASGRF2* stimulate the conversion of the GDP-bound form into the active form. However, the methylation changes in our experiment of *RASGRF2* were contrary to the changes expected if the H-Ras pathway were activated. *RASGRF2* expression has been shown to be nuclear in lung cancer, but little is known about the role of *RASGRF2* expression during carcinogenesis. Ras GAP protein generates potent anti-apoptotic signals after cleavage by caspase and may play an anti-apoptotic role in tumor cell lines (15,16). Whether *RASGRF2* acts as a TSG by activating apoptotic signals, as well as activating the K-*ras* gene, is unknown and requires further study.

Inactivation of TSGs may occur via multiple mechanisms, including allelic loss, gene mutation, or by methylation of CpG sites in promoter regions. *RASSF1A* is frequently silenced in lung cancer due to promoter hypermethylation in a few studies, while the mutations of *RASSF1A* are rare. The frequency of *RASSF1A* promoter hypermethylation is about 70-100% in SCLC tumors whereas it is 30-60% in NSCLC samples (14). We found hypermethylation of *RASSF1A* in 100% (4/4) of SCLC and 70% (7/10) of NSCLC cell lines, in 39% (44/114) of primary tumors and none in corresponding non-malignant tissue. The results were highly consistent with the previous reports (14). We did not examine the expression of *RASSF1A* because it was confirmed by the previous study (17). However, there was no correlation between *RASSF1A* and *RASGRF2* methylation status. The reason might be that *RASSF1A* is one of the Ras-effectors, whereas *RASGRF2* regulate the RAS GTPases cycle.

Neither *RASGRF2* nor *RASSF1A* showed a significant association with methylation and patients' clinical characteristics. The prognostic association of *RASSF1A* methylation in lung cancer is a controversial issue (18-20). The lack of significance in the association of methylation with the outcome may result from the limited number of patients in our study or other factors. However, the frequent methylation of *RASGRF2* and *RASSF1A* genes in lung cancer, without any correlation with clinical factors, would suggest that inactivation of these genes might be a ubiquitous mechanism stimulating tumor cell growth, rather than a means of further subdividing tumors into constituent biological or prognostic groups.

In conclusion, we demonstrated frequent inactivation of the *RASGRF2* gene through aberrant methylation of the promoter in NSCLC cell lines. We also frequently found methylation of *RASGRF2* in primary NSCLC. Aberrant methylation of the *RASGRF2* gene appears to be an important factor in the pathogenesis of NSCLC, a different role compared to *RASSF1A*. Our findings of a frequent acquired tumor-related epigenetic alteration favor the candidacy of *RASGRF2* as a TSG.

Acknowledgments

This work was supported by a grant from Sasagawa Foundation Program. We thank Yusuke Suenaga, Biology Department, Faculty of Science, Chiba University, Japan, for preparing cDNA and its normalization. We greatly thank Dr Toshikazu Ushijima, Carcinogenesis Division, National Cancer Center Research Institute, Japan, for his technical advice.

References

1. Kohno T and Yokoto J: How many tumor suppressor genes are involved in human lung carcinogenesis? Carcinogenesis 20: 1403-1410, 1999.
2. Brauch H, Johnson B, Hovis J, Yano T, Gazdar A, Pettengill OS, Graziano S, Sorenson GD, Poiesz BJ and Minna J: Molecular analysis of the short arm of chromosome 3 in small cell and non-small cell carcinoma of the lung. N Engl J Med 317: 1109-1113, 1987.
3. Dammann R, Li C, Yoon JH, Chin PL, Bates S and Pfeifer GP: Epigenetic inactivation of a RAS association domain family protein from the lung tumour suppressor locus 3p21.3. Nat Genet 25: 315-319, 2000.
4. Pfeifer GP, Yoon JH, Liu L, Tommasi S, Wilczynski SP and Dammann R: Methylation of the RASSF1A gene in human cancers. Biol Chem 383: 907-914, 2002.
5. Burbee DG, Forgacs E, Zochbauer-Muller S, Shivakumar L, Fong K, Gao B, Randle D, Kondo M, Virmani A, Bader S, Sekido Y, Latif F, Milchgrub S, Toyooka S, Gazdar AF, Lerman MI, Zabarovsky E, White M and Minna JD: Epigenetic inactivation of RASSF1A in lung and breast cancers and malignant phenotype suppression. J Natl Cancer Inst 93: 691-699, 2001.
6. Ortiz-Vega S, Khokhlatchev A, Nedwidek M, Zhang XF, Dammann R, Pfeifer GP and Avruch J: The putative tumor suppressor RASSF1A homodimerizes and heterodimerizes with the Ras-GTP binding protein Nore1. Oncogene 21: 1381-1390, 2002.
7. Shivakumar L, Minna J, Sakamaki T, Pestell R and White MA: The RASSF1A tumor suppressor blocks cell cycle progression and inhibits cyclin D1 accumulation. Mol Cell Biol 22: 309-318, 2002.
8. Anborgh PH, Qian X, Papageorge AG, Vass WC, deClue JE and Lowy DR: Ras-specific exchange factor GRF: oligomerization through its Dbl homology domain and calcium-dependent activation of Raf. Mol Cell Biol 19: 4611-4622, 1999.
9. Arozarena I, Matallanas D, Berciano MT, Sanz-Moreno V, Calvo F, Munoz MT, Egea G, Lafarga M and Crespo P: Activation of H-Ras in the endoplasmic reticulum by the RasGRF family guanine nucleotide exchange factors. Mol Cell Biol 24: 1516-1530, 2004.
10. Qiu C, Yu M, Shan L and Snyderwine EG: Allelic imbalance and altered expression of genes in chromosome 2q11-2q16 from rat mammary gland carcinomas induced by 2-amino-1-methyl-6-phenylimidazo[4,5-b]pyridine. Oncogene 22: 1253-1260, 2003.
11. Hagihara A, Miyamoto K, Furuta J, Hiraoka N, Wakazono K, Seki S, Fukushima S, Tsao MS, Sugimura T and Ushijima T: Identification of 27 5' CpG islands aberrantly methylated and 13 genes silenced in human pancreatic cancers. Oncogene 23: 8705-8710, 2004.
12. Girard L, Zochbauer-Muller S, Virmani AK, Gazdar AF and Minna JD: Genome-wide allelotyping of lung cancer identifies new regions of allelic loss, differences between small cell lung cancer and non-small cell lung cancer, and loci clustering. Cancer Res 60: 4894-4906, 2000.
13. Suzuki M, Toyooka S, Miyajima K, Iizasa T, Fujisawa T, Bekele NB and Gazdar AF: Alterations in the mitochondrial displacement loop in lung cancers. Clin Cancer Res 9: 5636-5641, 2003.
14. Zochbauer-Muller S, Minna JD and Gazdar AF: Aberrant DNA methylation in lung cancer: biological and clinical implications. Oncologist 7: 451-457, 2002.
15. Leblanc V, Delumeau I and Tocque B: Ras-GTPase activating protein inhibition specifically induces apoptosis of tumour cells. Oncogene 18: 4884-4889, 1999.
16. Yang JY and Widmann C: The RasGAP N-terminal fragment generated by caspase cleavage protects cells in a Ras/PI3K/Akt-dependent manner that does not rely on NFkappa B activation. J Biol Chem 277: 14641-14646, 2002.
17. Suzuki M, Sunaga N, Shames DS, Toyooka S, Gazdar AF and Minna JD: RNA interference-mediated knockdown of DNA methyltransferase 1 leads to promoter demethylation and gene re-expression in human lung and breast cancer cells. Cancer Res 64: 3137-3143, 2004.
18. Tomizawa Y, Kohno T, Kondo H, Otsuka A, Nishioka M, Niki T, Yamada T, Maeshima A, Yoshimura K, Saito R, Minna JD and Yokota J: Clinicopathological significance of epigenetic inactivation of RASSF1A at 3p21.3 in stage I lung adenocarcinoma. Clin Cancer Res 8: 2362-2368, 2002.
19. Wang J, Lee JJ, Wang L, Liu DD, Lu C, Fan YH, Hong WK and Mao L: Value of p16INK4a and RASSF1A promoter hypermethylation in prognosis of patients with resectable non-small cell lung cancer. Clin Cancer Res 10: 6119-6125, 2004.
20. Toyooka S, Suzuki M, Maruyama R, Toyooka KO, Tsukuda K, Fukuyama Y, Iizasa T, Aoe M, Date H, Fujisawa T, Shimizu N and Gazdar AF: The relationship between aberrant methylation and survival in non-small cell lung cancers. Br J Cancer 91: 771-774, 2004.

Available online at www.sciencedirect.com
SCIENCE DIRECT
ELSEVIER
Biochemical and Biophysical Research Communications 347 (2006) 327–333
BBRC
www.elsevier.com/locate/ybbrc

p73-dependent induction of 14-3-3σ increases the chemo-sensitivity of drug-resistant human breast cancers

Meixiang Sang [a,b], Yuanyuan Li [a], Toshinori Ozaki [a], Sayaka Ono [c], Kiyohiro Ando [a], Hideki Yamamoto [a], Tadayuki Koda [c], Cuizhi Geng [b], Akira Nakagawara [a,*]

[a] *Division of Biochemistry, Chiba Cancer Center Research Institute, Chiba 260-8717, Japan*
[b] *The First Surgery, Graduate School of Hebei Medical University, Hebei 050017, PR China*
[c] *Center for Functional Genomics, Hisamitsu Pharmaceutical Co., Inc., Chiba 260-8717, Japan*

Received 10 June 2006
Available online 21 June 2006

Abstract

It has been well documented that tumor suppressor *p53* is mutated in about 50% of all human tumors. *p53* status might be one of the critical determinants for the chemo-sensitivity of human tumors. In the present study, we have found that p53 family member p73 as well as 14-3-3σ is down-regulated in response to adriamycin (ADR) in ADR-resistant human breast cancer-derived MBA-MD-436 cells which carry *p53* mutation. Like p53, *14-3-3σ* was transactivated by p73 and, in turn, stabilized p73. Luciferase reporter analysis and colony formation assays demonstrated that 14-3-3σ has an ability to enhance the p73-mediated transcriptional activity as well as its pro-apoptotic function. Furthermore, enforced expression of 14-3-3σ increased the ADR sensitivity of MBA-MD-436 cells. Taken together, our present results strongly suggest that p73-dependent induction of 14-3-3σ plays an important role in the regulation of chemo-sensitivity of breast cancers bearing *p53* mutation.

Keywords: Adriamycin; Breast cancer; 14-3-3σ; p53; p73

The tumor suppressor *p53* which encodes a sequence-specific nuclear transcription factor is the most frequently mutated gene in human cancers [1]. Mounting evidence showed that p53 is induced to be accumulated in response to various cellular stresses such as DNA damage, and thereby exerts its pro-apoptotic function through the transactivation of the p53-target genes implicated in the regulation of the apoptotic cell death including *Bax*, *Noxa*, *Puma*, and *p53AIP1* [2–5]. Newly identified p53 family members, p73 and p63, promote cell cycle arrest and/or apoptosis similarly to p53 [6–10]. Although *p73* and *p63* are rarely mutated in human cancers [11], it has been shown that they are required for the p53-mediated apoptosis in response to DNA damage [12]. Since cancer cells which carry *p53* mutation are more resistant to chemotherapeutic agents than those with wild-type p53 [13,14], it is likely that p73 and/or p63 might contribute to sensitize p53-deficient cancer cells to chemotherapeutic agents.

About 30–50% of human breast cancers express mutant forms of p53 [15,16]. Additionally, Moll et al. found that the pro-apoptotic function of wild-type p53 expressed in about 30% of human breast cancers is inhibited due to its aberrant cytoplasmic localization [17]. 14-3-3σ, which is one of the 14-3-3 family members, has been initially identified as a human mammary epithelium-specific marker 1 [18]. Intriguingly, the expression of 14-3-3σ is undetectable in most breast cancers due to the hypermethylation of CpG islands in the *14-3-3σ* gene [19]. Enforced expression of 14-3-3σ suppresses the anchorage-independent growth of several breast cancer cell lines [20]. Alternatively, it has been shown that 14-3-3σ is strongly induced in response to DNA damage, and its expression is directly regulated by

* Corresponding author. Fax: +81 43 265 4459.
E-mail address: akiranak@chiba-cc.jp (A. Nakagawara).

0006-291X/$ - see front matter © 2006 Elsevier Inc. All rights reserved.
doi:10.1016/j.bbrc.2006.06.079

p53 [21]. Yang et al. described that 14-3-3σ stabilizes p53 and enhances its transcriptional activity through the interaction with p53, suggesting that 14-3-3σ has a positive feedback effect on p53 [22].

In the present study, we have found that the adriamycin (ADR)-resistant phenotype of certain human breast cancer cells with *p53* mutation is significantly associated with the down-regulation of 14-3-3σ as well as p73. Of note, *14-3-3σ* was transactivated by p73, and enhanced its transcriptional and pro-apoptotic activity. Thus, it is likely that p73/14-3-3σ pathway plays an important role in the regulation of DNA damage-induced apoptosis in certain breast cancer cells bearing *p53* mutation.

Materials and methods

Cell culture and transfection. COS7 and human breast cancer-derived cell lines were maintained in Dulbecco's modified Eagle's medium (DMEM) supplemented with 10% heat-inactivated fetal bovine serum (FBS, Invitrogen) and antibiotic mixture. p53-deficient human lung carcinoma H1299 cells were grown in RPMI 1640 medium plus 10% heat-inactivated FBS and antibiotic mixture. Cultures were grown at 37 °C in a water-saturated atmosphere of 5% CO_2 in air. For transfection, cells were transfected with the indicated combinations of the expression plasmids using LipofectAMINE 2000 transfection reagent according to the manufacturer's recommendations (Invitrogen).

MTT assays. Cells were seeded at a cell density of 5000 cells/well in 96-well tissue culture plates. After attachment overnight, cells were exposed to adriamycin (ADR) at a final concentration of 1 μM for the indicated time periods. MTT assays were performed as described previously [23]. In brief, 10 μl of MTT solution was added to each well. After one hour of incubation at 37 °C, the absorbance readings for each well were carried out at 570 nm using the microplate reader (Bio-Rad).

TUNEL assays. Transfected cells were exposed to ADR at a final concentration of 1 μM for 24 h. Apoptotic cells were identified using an *in situ* cell detection, peroxidase kit (Roche Applied Science). In brief, cells were washed with ice-cold PBS and fixed in 4% paraformaldehyde for 1 h. Cells were then permeabilized with 0.1% Triton X-100 in 0.1% sodium citrate for 2 min on ice and washed with PBS. The labeling reaction was performed using TMR red-labeled dUTP together with other nucleotides by terminal deoxynucleotidyl transferase for 1 h in the dark at 37 °C in a humidified chamber. Then cells were washed with PBS, mounted, and the incorporated TMR red-labeled dUTP was analyzed using a Fluoview laser scanning confocal microscope (Olympus).

RT-PCR. Total RNA was extracted from the indicated cell lines by using RNeasy Mini Kit (Qiagen) according to the manufacturer's protocol. cDNA was generated from 1 μg of total RNA using random primers and SuperScript II reverse transcriptase (Invitrogen). PCR-based amplification was performed using the cDNA as a template with the following primers: *p73* forward, 5′-TGGAACCAGACAGCACCTACTTCG-3′ and *p73* reverse, 5′-TGCTGGAAAGTGACCTCAAAGTGG-3′; $p21^{WAF1}$ forward, 5′-ATGAAATTCACCCCCTTTCC-3′ and $p21^{WAF1}$ reverse, 5′-CCCTAATCACCTGCCTGACCATTCCACCAAGG-3′; *erbB2* forward, 5′-GGGCTGGCCCGATGTATTTGAT-3′ and *erbB2* reverse, 5′-ATAGAGGTTGTCGAAGGCTGGGC3′; *Noxa* forward, 5′-CTGGAAGTCGAGTGTGCTACT-3′ and *Noxa* reverse, 5′-TCAGGTTCCTGAGCAGAAGAG-3′; *14-3-3σ* forward, 5′-GAGCGAAACCTGCTCTCAGT-3′ and *14-3-3σ* reverse, 5′-CTCCTTGATGAGGTGGCTGT-3′; *GAPDH* forward, 5′-ACCTGACCTGCCGTCTAGAA-3′ and *GAPDH* reverse, 5′-TCCACCACCCTGTTGCTGTA-3′. PCR products were separated on 2% agarose gel electrophoresis and visualized by ethidium bromide staining.

Immunoblotting. Whole cell lysates were separated on 10% SDS–PAGE and transferred onto a polyvinylidene difluoride membrane (Millipore). The membrane was blocked with TBS (50 mM Tris–HCl, pH 8.0, 100 mM NaCl and 0.1% Tween 20) containing 5% nonfat dried milk, and then probed with the monoclonal anti-p73 (Ab-4, NeoMarkers), monoclonal anti-erbB2 (3B5, Calbiochem), polyclonal anti-14-3-3σ (C-18, Santa Cruz Biotechnology), polyclonal anti-Noxa (Zymed), or with polyclonal anti-actin (20-33, Sigma) antibody. The immunoreactive bands were visualized by using HRP-conjugated anti-mouse or anti-rabbit IgG antibody (Jackson ImmunoResearch Laboratories) and ECL (Amersham Biosciences).

Immunoprecipitation. Whole cell lysates prepared from MBA-MD-436 cells treated with or without ADR were immunoprecipitated with the monoclonal anti-p73 followed by immunoblotting with the anti-p73 antibody.

Protein decay rate analysis. COS7 cells were transiently transfected with the indicated combinations of the expression plasmids. Twenty-four hours after transfection, cells were exposed to cycloheximide (Sigma) at a final concentration of 100 μg/ml. At the indicated time points after the treatment with cycloheximide, cells were harvested and subjected to immunoblotting with the anti-p73 or with the anti-actin antibody.

Luciferase reporter assay. p53-deficient H1299 cells were transiently transfected with 100 ng of the p53/p73-responsive luciferase reporter plasmid ($p21^{WAF1}$ or *BAX*), 10 ng of pRL-TK *Renilla* luciferase cDNA, and 25 ng of the expression plasmid for HA-p73α together with or without the increasing amounts of the expression plasmid encoding 14-3-3σ. Total amounts of plasmid DNA were kept constant (510 ng) with pcDNA3 (Invitrogen) per transfection. Forty-eight hours after transfection, both firefly and *Renilla* luciferase activities were measured by the dual-luciferase reporter assay system according to the manufacturer's instructions (Promega). The firefly luminescence signal was normalized based on the *Renilla* luminescence signal. The results were obtained from at least three sets of transfection and presented as means ± SD.

Colony formation assay. H1299 cells were seeded at a cell density of 2×10^5 cells/well in 6-well tissue culture plates and transfected with the indicated combinations of the expression plasmids. Forty-eight hours after transfection, cells were selected with G418 (at a final concentration of 400 μg/ml) for 2 weeks. The surviving colonies were fixed in methanol and stained with Giemsa's solution.

Results

ADR sensitivity and expression of p53-related genes in human breast cancer-derived cell lines

To examine the adriamycin (ADR) sensitivity of the human breast cancer-derived cell lines including MCF-7, MDA-MB-231, and MDA-MB-436, these cells were treated with 1 μM of ADR for the indicated time periods, and their viabilities were analyzed by the standard MTT assay. ADR has been considered as a mandatory agent in breast cancer chemotherapy [24]. As described previously [25], MCF-7 cells carry wild-type p53, whereas MDA-MB-231 and MDA-MB-436 cells express mutant form of p53. As shown in Fig. 1A, MCF-7 and MDA-MB-231 cells underwent apoptotic cell death in response to ADR, whereas MDA-MB-436 cells showed an ADR-resistant phenotype, which was also supported by FACS analysis (data not shown). Consistent with the previous observations [1], p53 was induced to be accumulated at protein level in MCF-7 cells exposed to ADR in association with the up-

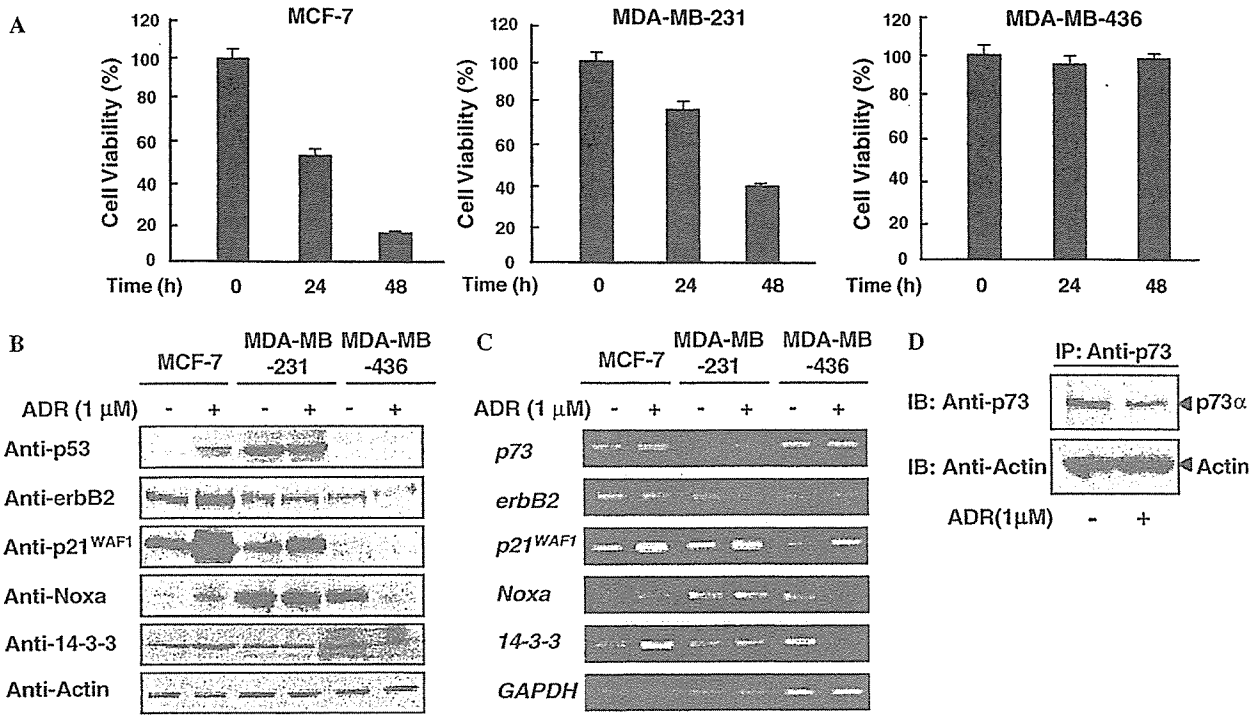

Fig. 1. The expression of *p53*-related genes in breast cancer cells in response to ADR. (A) Cell survival assays. Human breast cancer-derived MCF-7, MDA-MB-231, and MDA-MB-436 cells were exposed to ADR (at a final concentration of 1 μM). At the indicated time periods after the treatment with ADR, cell viability was examined by standard MTT assay. (B) Immunoblotting. MCF-7, MDA-MB-231, and MDA-MB-436 cells were treated with ADR (at a final concentration of 1 μM) or left untreated. Whole cell lysates were prepared and processed for immunoblotting with the indicated antibodies. Immunoblotting for actin is shown as control for protein loading. (C) RT-PCR analysis. MCF-7, MDA-MB-231, and MDA-MB-436 cells were treated with ADR as in (B). Twenty-four hours after the treatment, total RNA was prepared and subjected to RT-PCR for the expression of *p73*, *erbB2*, $p21^{WAF1}$, *Noxa* and *14-3-3σ*. Amplification of *GAPDH* served as an internal control. (D) Immunoprecipitation. MDA-MB-436 cells were treated with 1 μM ADR or left untreated. Twenty-four hours after the treatment, whole cell lysates were immunoprecipitated with the monoclonal anti-p73 antibody followed by immunoblotting with the anti-p73 antibody.

regulation of its direct targets such as $p21^{WAF1}$, Noxa, and 14-3-3σ (Fig. 1B). In ADR-sensitive MDA-MB-231 cells, ADR-mediated increase in the amounts of $p21^{WAF1}$ was detectable, however, the expression levels of p53, Noxa, and 14-3-3σ remained unchanged regardless of ADR treatment, suggesting that ADR-mediated apoptotic cell death in MDA-MB-231 cells might be regulated in a p53-independent manner. In a sharp contrast to MCF-7 and MDA-MB-231 cells, p53 was undetectable under our experimental conditions, and ADR-dependent down-regulation of Noxa and 14-3-3σ was observed in ADR-resistant MDA-MB-436 cells. Similar results were also obtained in RT-PCR analysis (Fig. 1C). *p73* as well as *erbB2* mRNA level remained almost constant regardless of ADR treatment. In addition, ADR had no detectable effects of the expression levels of *p53* mRNA (data not shown). Of note, immunoprecipitation experiments demonstrated that p73 is reduced in MDA-MB-436 cells exposed to ADR (Fig. 1D), whereas p73 levels remained unchanged in MCF-7 and MBA-MD-231 cells regardless of ADR treatment (data not shown), indicating that ADR-mediated down-regulation of Noxa and 14-3-3σ could be due to the down-regulation of p73, and also suggesting that p73 could play an important role in the regulation of ADR sensitivity in certain breast cancer cells bearing *p53* mutation.

14-3-3σ is a direct target of p73 and increases its stability

Since Noxa has been shown to be a direct transcriptional target of p53 as well as p73, and play a critical role in the regulation of p53/p73-mediated apoptotic cell death [9], we focused our attention on the possible link between p73 and 14-3-3σ. Recently, Yang et al. demonstrated that 14-3-3σ is a direct transcriptional target of p53 and increases its stability [22]. Thus, we sought to examine whether p73 could transactivate *14-3-3σ* in cells. COS7 cells were transiently transfected with the expression plasmid for HA-p73α or p53. Forty-eight hours after transfection, total RNA was prepared and subjected to RT-PCR analysis. As shown in Fig. 2A, HA-p73α as well as p53 enhanced the transcription of the endogenous *14-3-3σ*. Similar results were also obtained in immunoblotting (Fig. 2B). Next, we examined the possible effect of 14-3-3σ on the stability of p73α. To this end, p53-deficient H1299 cells were transiently co-transfected with the constant amount of the HA-p73α expression plasmid along with or without the increasing amounts of the expression plasmid for 14-3-3σ. As seen

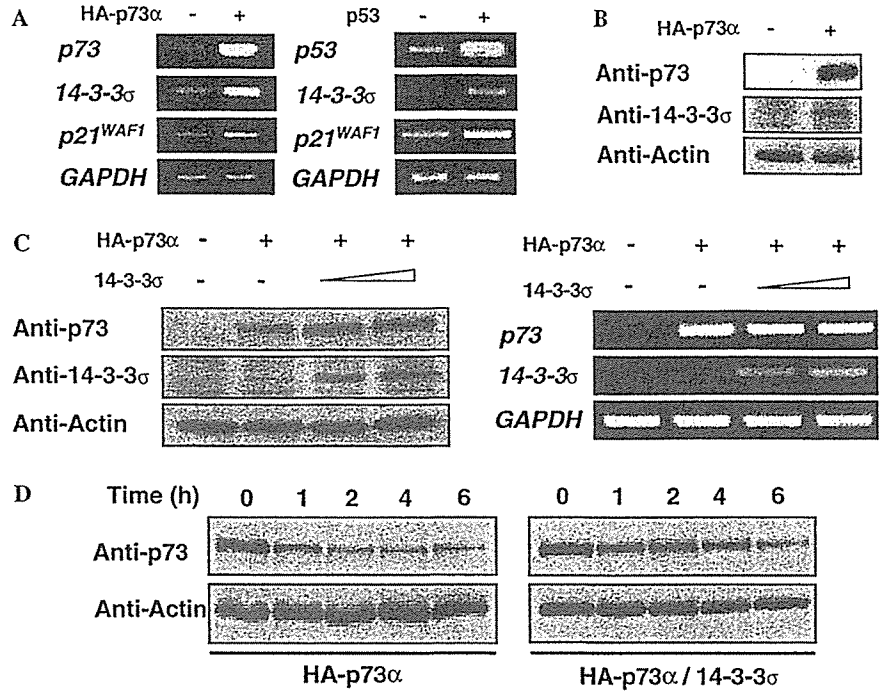

Fig. 2. *14-3-3σ* is a transcriptional target of p73 and increases its stability. (A) p73-mediated up-regulation of 14-3-3σ. COS7 cells were transiently transfected with the expression plasmid for HA-p73α (left panel) or p53 (right panel). Forty-eight hours after transfection, total RNA was prepared and subjected to RT-PCR. (B) Immunoblotting. p53-deficient H1299 cells were transiently transfected with the empty plasmid or with the expression plasmid encoding HA-p73α. Forty-eight hours after transfection, whole cell lysates were prepared and subjected to immunoblotting with the indicated antibodies. (C) 14-3-3σ stabilizes p73. H1299 cells were transiently co-transfected with the constant amount of HA-p73α expression plasmid together with or without the increasing amounts of the expression plasmid for 14-3-3σ. Forty-eight hours after transfection, whole cell lysates and total RNA were analyzed by immunoblotting with the indicated antibodies and RT-PCR, respectively. (D) A half-life of p73 in the presence of 14-3-3σ. H1299 cells were transiently transfected with the HA-p73α expression plasmid alone or with the HA-p73α expression plasmid plus 14-3-3σ expression plasmid. Twenty-four hours after transfection, cells were exposed to cycloheximide (at a final concentration of 100 μg/ml). At the indicated time points after the addition of cycloheximide, whole cell lysates were analyzed for HA-p73α. Actin was used for equal protein loading.

in Fig. 2C, 14-3-3σ increased the amounts of HA-p73α in a dose-dependent manner, whereas 14-3-3σ had undetectable effect on the *p73α* mRNA level, suggesting that 14-3-3σ has an ability to stabilize p73 in cells. To further confirm this notion, we measured a half-life of p73α in the presence or absence of the exogenous 14-3-3σ using cycloheximide blockade. As seen in Fig. 2D, a half-life of p73α was prolonged in the presence of 14-3-3σ as compared with that of p73α alone. Taken together, our present results strongly suggest that, like p53, 14-3-3σ is a direct transcriptional target of p73 and stabilizes p73.

14-3-3σ enhances the p73-mediated transcriptional activity as well as pro-apoptotic function

To address whether 14-3-3σ could affect the p73 function, we performed the luciferase reporter assays. For this purpose, H1299 cells were transiently co-transfected with the constant amount of the p73α expression plasmid and the p53/p73-responsive luciferase reporter construct carrying the $p21^{WAF1}$ or *Bax* promoter together with or without the increasing amounts of the expression plasmid for 14-3-3σ. Forty-eight hours after transfection, cells were harvested and their luciferase activities were measured. As expected, 14-3-3σ enhanced the p73α-mediated transactivation toward $p21^{WAF1}$ and *Bax* promoters in a dose-dependent manner (Fig. 3A). Next, we examined whether 14-3-3σ could enhance the p73-mediated apoptosis. H1299 cells were transfected with the empty plasmid, HA-p73α expression plasmid, or with the HA-p73α expression plasmid plus 14-3-3σ expression plasmid. Forty-eight hours after transfection, cells were transferred to the fresh medium containing G418. After 2 weeks of selection, G418-resistant colonies were stained with Giemsa's solution. As shown in Fig. 3B, the number of G418-resistant colonies was significantly reduced in cells co-expressing HA-p73α and 14-3-3σ as compared with that in cells expressing HA-p73α alone. Thus, we concluded that 14-3-3σ has an ability to enhance the p73 function through the stabilization of p73.

Enforced expression of 14-3-3σ increases the ADR sensitivity of ADR-resistant MDA-MB-436 cells

To ask whether 14-3-3σ could affect the ADR sensitivity in ADR-resistant MDA-MB-436 cells, MDA-MB-436 cells were transfected with the empty plasmid (436-C) or with the expression plasmid for 14-3-3σ (436-14), and maintained in the presence of G418. Two weeks of selection,

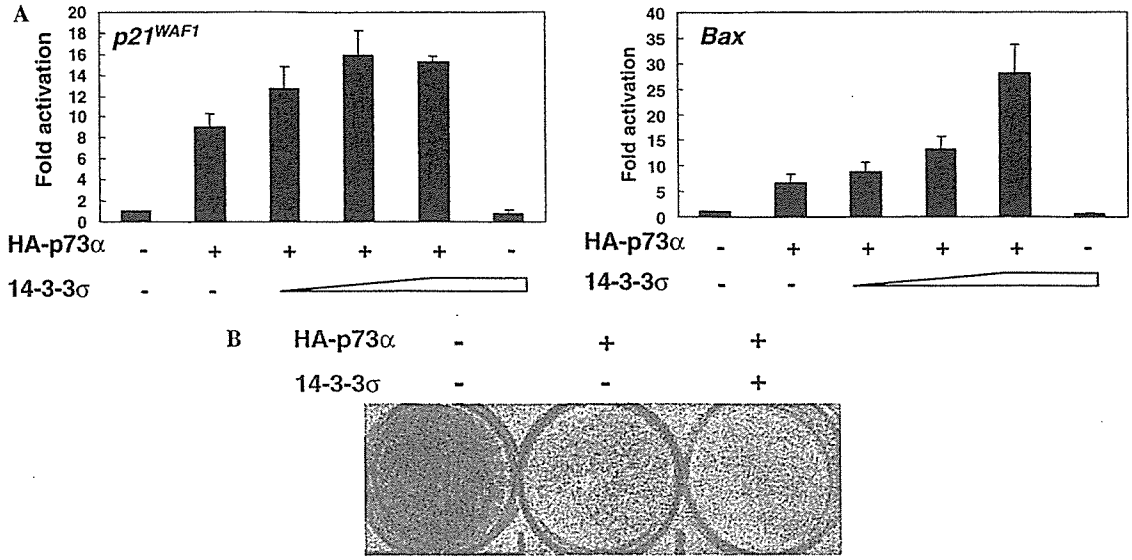

Fig. 3. *14-3-3σ* enhances the p73-mediated transcription as well as apoptosis. (A) Luciferase reporter assay. H1299 cells were transiently co-transfected with the constant amounts of the expression plasmid for HA-p73α, p53/p73-responsive luciferase reporter construct containing the $p21^{WAF1}$ (left panel) or *Bax* (right panel) promoter, *Renilla* luciferase reporter together with or without the increasing amounts of the expression plasmid for 14-3-3σ. Forty-eight hours after transfection, luciferase activities were measured as described under "Materials and methods". (B) Colony formation assay. H1299 cells were transfected with empty plasmid, the expression plasmid for HA-p73α or with the expression plasmid for HA-p73α plus 14-3-3σ expression plasmid. Forty-eight hours after transfection, cells were transferred to the fresh medium containing G418 (at a final concentration of 400 μg/ml). After 2 weeks of selection, drug-resistant colonies were fixed and stained with Giemsa's solution.

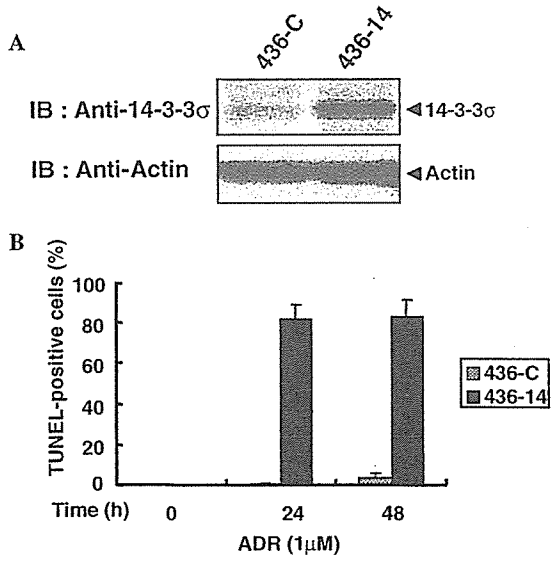

Fig. 4. Effects of 14-3-3σ on the ADR sensitivity in MDA-MB-436 cells. (A) Enforced expression of 14-3-3σ in MDA-MB-436 cells. MDA-MB-436 cells were transfected with the empty plasmid (436-C) or with the expression plasmid for 14-3-3σ (436-14). Forty-eight hours after transfection, cells were transferred to the fresh medium containing 400 μg/ml G418. After 2 weeks of selection, surviving cells were harvested and then whole cell lysates were subjected to immunoblotting with the indicated antibodies. (B) TUNEL assay. Control MDA-MB-436 cells (436-C) and MDA-MB-436 cells expressing 14-3-3σ (436-14) were exposed to ADR (at a final concentration of 1 μg/ml) or left untreated. Twenty-four and Forty-eight hours after the treatment with ADR, apoptotic cell death was examined by TUNEL assay.

whole cell lysates were prepared from the surviving cells and subjected to immunoblotting. As shown in Fig. 4A, the increased expression of 14-3-3σ was observed in cells transfected with 14-3-3σ expression plasmid. We then examined the ADR sensitivity by TUNEL assays. As seen in Fig. 4B, the number of MDA-MB-436 cells expressing 14-3-3σ with apoptotic nuclei was significantly increased in response to ADR as compared with that of the control MDA-MB-436 cells. Collectively, our present results strongly suggest that p73/14-3-3σ pathway plays an important role in the regulation of the chemo-sensitivity of certain breast cancer cells bearing *p53* mutation.

Discussion

Mammalian 14-3-3 protein family comprises at least seven isoforms. Among them, *14-3-3σ* is mapped at human chromosome 1p35, a region which shows frequent loss of heterozygosity in a wide variety of human cancers including breast cancers [21,26]. Indeed, the expression levels of *14-3-3σ* were significantly lower in breast cancers than those in normal breast epithelium, which might be due to the hypermethylation of CpG islands in the *14-3-3σ* gene locus [19], and an enforced expression of 14-3-3σ inhibited the oncogene-activated tumorigenesis [27]. Intriguingly, 14-3-3σ was transactivated by p53 in response to DNA damage [21], and positively regulated its activity [22], indicating that there exists a positive feedback regulation of p53 by its target 14-3-3σ. In the present study, we have found that 14-3-3σ is a direct

transcriptional target of p73 and enhances the p73-mediated transcriptional as well as pro-apoptotic activity. Furthermore, an enforced expression of 14-3-3σ in ADR-resistant human breast cancer MDA-MB-436 cells bearing *p53* mutation resulted in an increased cell killing by ADR. Collectively, our present results strongly suggest that p73/14-3-3σ pathway plays an important role in the regulation of chemo-sensitivity in certain breast cancer cells bearing *p53* mutation.

According to the results described by Yang et al. 14-3-3σ had an ability to increase the stability and the transcriptional activity of p53 through the physical interaction with p53 [22]. They also demonstrated that 14-3-3σ inhibits the MDM2-mediated p53 ubiquitination and nuclear export. In spite of our extensive efforts, we could not detect the physical interaction between p73α and 14-3-3σ under our experimental conditions (data not shown). Although it might be due to the different cell systems used in our immunoprecipitation experiments, it is likely that 14-3-3σ-mediated increase in the stability and activity of p73α could be regulated by a still unknown indirect mechanism(s). Recently, Rossi et al. reported that a HECT-type E3 ubiquitin protein ligase Itch binds to and ubiquitinates p73, and thereby promoting its rapid proteasome-dependent degradation [28]. They also described that the expression levels of Itch are down-regulated in cells in response to DNA damage. Since 14-3-3σ induced the degradation of MDM2 [22], it is tempting to speculate that E3 ubiqitin protein ligase activity of Itch could be blocked by 14-3-3σ. This issue is currently under investigation.

According to the previous results, p73 was induced to be accumulated at protein level in response to ADR treatment and thereby promoting apoptotic cell death [29,30]. In a sharp contrast, p53/p73-target genes such as *Noxa* and *14-3-3σ* were significantly down-regulated following ADR treatment in ADR-resistant MDA-MB-436 cells. MCF-7 cells carrying wild-type p53 underwent apoptosis in response to ADR in a p53-dependent manner. Since MDA-MB-436 cells express nonfunctional p53 [25], it is possible that the ADR-mediated upstream activation pathways including the post-translational modifications such as phosphorylation and acetylation which regulate p73 function [9,10] might be disrupted in these cells. Based on our present results, enforced expression of 14-3-3σ in p53-deficient H1299 cells enhanced the p73-mediated apoptotic cell death as examined by colony formation assay. Furthermore, the ADR sensitivity of MDA-MB-436 cells was increased in the presence of exogenously expressed 14-3-3σ. Thus, it is likely that p73/14-3-3σ-mediated apoptotic pathway might be one of the critical determinants of cell fate in response to ADR in certain breast cancer cells bearing *p53* mutation, and that p73 might be effective in p53-deficient breast cancer cells which are resistant to anti-cancer drug. In this connection, further work is required to determine how the ADR-mediated activation of p73 is blocked in MDA-MB-436 cells.

Acknowledgments

This work was supported in part by a Grant-in-Aid from the Ministry of Health, Labor and Welfare for Third Term Comprehensive Control Research for Cancer, a Grant-in-Aid for Scientific Research on Priority Areas from the Ministry of Education, Culture, Sports, Science and Technology, Japan, and a Grant-in-Aid for Scientific Research from Japan Society for the Promotion of Science.

References

[1] K.H. Vousden, X. Lu, Live or death: the cells response to p53, Nat. Rev. Cancer 2 (2002) 594–604.
[2] T. Miyashita, J.C. Reed, Tumor suppressor p53 is a direct transcriptional activator of the human bax gene, Cell 80 (1995) 293–299.
[3] E. Oda, R. Ohki, H. Murasawa, J. nemoto, T. Shibue, T. Yamashita, T. Tokino, T. Taniguchi, N. Tanaka, Noxa, a BH3-only member of the Bcl-2 family and candidate mediator of p53-induced apoptosis, Science 288 (2000) 1053–1058.
[4] J. Yu, L. Zhang, P.M. Hwang, K.W. Kinzler, B. Vogelstein, PUMA induces the rapid apoptosis of colorectal cancer cells, Mol. Cell 7 (2001) 673–682.
[5] K. Oda, H. Arakawa, T. Tanaka, K. matsuda, C. Tanikawa, T. Mori, H. Nishimori, K. Tamai, T. Tokino, Y. Nakamura, Y. Taya, p53AIP1, a potential mediator of p53-dependent apoptosis, and its regulation by Ser-46- phosphorylated p53, Cell 102 (2000) 849–862.
[6] M. Kaghad, H. Bonnet, A. Yang, L. Creancier, J.C. Biscan, A. Valent, A. Minty, P. Chalon, J.M. Lelias, X. Dumont, P. Ferrara, F. McKeon, D. Caput, Monoallelically expressed gene related to p53 at 1p36, a region frequently deleted in neuroblastoma and other human cancers, Cell 90 (1997) 809–819.
[7] M. Osada, M. Ohba, C. Kawahara, C. Ishioka, R. Kanamaru, I. Kato, Y. Ikawa, Y. Nimura, A. Nakagawara, M. Obinata, S. Ikawa, Cloning and functional analysis of human p51, which structurally and functionally resembles p53, Nat. Med. 4 (1998) 839–843.
[8] A. Yang, M. Kaghad, Y. Wang, E. Gillett, M.D. Fleming, V. Dotsch, N.C. Andrews, D. Caput, F. McKeon, p63, a p53 homolog at 3q27-29, encodes multiple products with transactivating, death-inducing, and dominant-negative activities, Mol. Cell 2 (1998) 305–316.
[9] G. Melino, V. De Laurenzi, K.H. Vousden, p73: friend or foe in tumorigenesis, Nat. Rev. Cancer 2 (2002) 605–615.
[10] T. Ozaki, A. Nakagawara, p73, a sophisticated p53 family member in the cancer world, Cancer Sci. 96 (2005) 729–737.
[11] S. Ikawa, A. Nakagawara, Y. Ikawa, p53 family genes: structural comparison, expression and mutation, Cell Death Differ. 6 (1999) 1154–1161.
[12] E.R. Flores, K.Y. Tsai, D. Crowley, S. Sengupta, A. Yang, F. McKeon, T. Jacks, p63 and p73 are required for p53-dependent apoptosis in response to DNA damage, Nature 416 (2002) 560–564.
[13] D. Gallardo, K.E. Drazan, W.H. McBride, Adenovirus-based transfer of wild-type p53 gene increases ovarian tumor radiosensitivity, Cancer Res. 56 (1996) 4891–4893.
[14] T. Mukhopadhyay, J.A. Roth, Induction of apoptosis in human lung cancer cells after wild-type p53 activation by methoxyestradiol, Oncogene 14 (1997) 379–384.
[15] L.V. Crawford, D.C. Pim, P. Lamb, The cellular protein p53 in human tumours, Mol. Biol. Med. 2 (1984) 261–272.
[16] G. Cattoretti, F. Rilke, S. Andreola, L. D'Amato, D. Domenico, p53 in breast cancer, Int. J. Cancer 41 (1988) 178–183.
[17] U.M. Moll, G. Riou, A.J. Levine, Two distinct mechanisms alter p53 in breast cancer: mutation and nuclear exclusion, Proc. Natl. Acad. Sci. USA 89 (1992) 7262–7266.
[18] G.L. Prasad, E.M. Valverius, E. McDuffie, H.L. Cooper, Complementary DNA cloning of a novel epithelial cell marker protein,